University of Nebraska - Lincoln

# DigitalCommons@University of Nebraska - Lincoln

# The Vaccinia Virus (VACV) B1 and Cellular VRK2 Kinases Promote VACV Replication Factory Formation through Phosphorylation-Dependent Inhibition of VACV B12

Annabel T. Olson
*University of Nebraska - Lincoln*, aolson18@unl.edu

Zhigang Wang
*University of Nebraska - Lincoln*, zwang4@unl.edu

Annabel Olson
*University of Nebraska - Lincoln*, aolson18@huskers.unl.edu

Alexandria C. Linville
*University of Nebraska - Lincoln*, alexandria.linville@huskers.unl.edu

Brianna L. Bullard
*University of Nebraska - Lincoln*, bbullard@huskers.unl.edu

Follow this and additional works at: https://digitalcommons.unl.edu/virologypub

*See next page for additional authors*

Part of the Biological Phenomena, Cell Phenomena, and Immunity Commons, Cell and Developmental Biology Commons, Genetics and Genomics Commons, Infectious Disease Commons, Medical Immunology Commons, Medical Pathology Commons, and the Virology Commons

## Authors

Annabel T. Olson, Zhigang Wang, Annabel Olson, Alexandria C. Linville, Brianna L. Bullard, Eric A. Weaver, Clinton Jones, and Matthew S. Wiebe

AMERICAN SOCIETY FOR MICROBIOLOGY

Journal of
Virology®

# The Vaccinia Virus (VACV) B1 and Cellular VRK2 Kinases Promote VACV Replication Factory Formation through Phosphorylation-Dependent Inhibition of VACV B12

Amber B. Rico,[a,b] Zhigang Wang,[a] Annabel T. Olson,[a,c] Alexandria C. Linville,[a,c] Brianna L. Bullard,[a,c] Eric A. Weaver,[a,c] Clinton Jones,[d] (ID) Matthew S. Wiebe[a,b]

[a]Nebraska Center for Virology, University of Nebraska, Lincoln, Nebraska, USA
[b]School of Veterinary Medicine and Biomedical Sciences, University of Nebraska, Lincoln, Nebraska, USA
[c]School of Biological Sciences, University of Nebraska, Lincoln, Nebraska, USA
[d]Department of Veterinary Pathobiology, Oklahoma State University Center for Veterinary Health Sciences, Stillwater, Oklahoma, USA

**ABSTRACT** Comparative examination of viral and host protein homologs reveals novel mechanisms governing downstream signaling effectors of both cellular and viral origin. The vaccinia virus B1 protein kinase is involved in promoting multiple facets of the virus life cycle and is a homolog of three conserved cellular enzymes called vaccinia virus-related kinases (VRKs). Recent evidence indicates that B1 and VRK2 mediate a common pathway that is largely uncharacterized but appears independent of previous VRK substrates. Interestingly, separate studies described a novel role for B1 in inhibiting vaccinia virus protein B12, which otherwise impedes an early event in the viral lifecycle. Herein, we characterize the B1/VRK2 signaling axis to better understand their shared functions. First, we demonstrate that vaccinia virus uniquely requires VRK2 for viral replication in the absence of B1, unlike other DNA viruses. Employing loss-of-function analysis, we demonstrate that vaccinia virus's dependence on VRK2 is only observed in the presence of B12, suggesting that B1 and VRK2 share a pathway controlling B12. Moreover, we substantiate a B1/VRK2/B12 signaling axis by examining coprecipitation of B12 by B1 and VRK2. Employing execution point analysis, we reveal that virus replication proceeds normally through early protein translation and uncoating but stalls at replication factory formation in the presence of B12 activity. Finally, structure/function analyses of B1 and VRK2 demonstrate that enzymatic activity is essential for B1 or VRK2 to inhibit B12. Together, these data provide novel insights into B1/VRK signaling coregulation and support a model in which these enzymes modulate B12 in a phosphorylation-dependent manner.

**IMPORTANCE** Constraints placed on viral genome size require that these pathogens must employ sophisticated, yet parsimonious mechanisms to effectively integrate with host cell signaling pathways. Poxviruses are no exception and employ several methods to balance these goals, including encoding single proteins that impact multiple downstream pathways. This study focuses on the vaccinia virus B1 protein kinase, an enzyme that promotes virus replication at multiple phases of the viral lifecycle. Herein, we demonstrate that in addition to its previously characterized functions, B1 inhibits vaccinia virus B12 protein via a phosphorylation-dependent mechanism and that this function of B1 can be complemented by the cellular B1 homolog VRK2. Combined with previous data implicating functional overlap between B1 and an additional cellular B1 homolog, VRK1, these data provide evidence of how poxviruses can be multifaceted in their mimicry of cellular proteins through the consolidation of functions of both VRK1 and VRK2 within the viral B1 protein kinase.

**KEYWORDS** B1, B12, DNA replication, poxvirus, protein kinases, pseudokinases, vaccinia virus, virus-host interactions

**P**oxviruses are complex, enveloped viruses with large, double-stranded DNA ge-
nomes that infect invertebrate and vertebrate species, including humans. Unlike
most mammalian DNA viruses, poxviruses perform all stages of their viral replication
cycle in the host cell cytoplasm. Vaccinia virus (VACV), the prototypical poxvirus,
encodes ~200 proteins that contribute to viral propagation in the cytoplasm (1). The
large virally encoded proteomes of vaccinia virus and other poxviruses contribute to
their autonomy and have allowed for mechanistic insight into virology and cell biology
alike. Viral usurpation or mimicry of cellular proteins is a strategy utilized by poxvirus
proteins at key interfaces between viral and host signaling (2–5). Multiple studies
indicate that the vaccinia virus B1 Ser/Thr protein kinase is one such example of
poxvirus mimicry of a family of cellular proteins.

The vaccinia virus B1 kinase is expressed early during infection and promotes
multiple facets of the vaccinia virus life cycle (6–11). Genetic and biochemical investi-
gations of the B1 kinase using temperature-sensitive viruses (7, 9, 12–14) and a B1
deletion mutant virus (6, 15) have provided insights into the essential roles played by
B1 during vaccinia virus infection. Importantly, the severity of the phenotype resulting
from B1 mutant virus infections in those studies was cell type dependent and was
limited at the stages of DNA replication (13–17), intermediate transcription (7, 11), or
morphogenesis (9), signifying a function for B1 in promoting viral replication at each of
these steps. Explication of B1 mutant vaccinia virus infections demonstrated that B1
promotes replication by phosphorylating and inactivating the cellular host defense
protein b̲arrier to a̲utointegration f̲actor (BAF; encoded by the *BANF1* gene) (7, 8, 16),
which is otherwise capable of binding the viral genome and impeding its replication
and transcription. In addition to its activity as a poxviral restriction factor, BAF is
involved with multiple processes contributing to host and pathogen genomic integrity
(reviewed in references 18 to 20). To date, overcoming BAF is foremost among the roles
of the vaccinia virus B1 kinase.

While B1 has been shown to be critical for vaccinia virus replication in every cell line
tested, the cell type-dependent severity of the mutant B1 phenotype indicated that the
functional activity of B1 and/or its substrates may be impacted by complementing host
kinases. Indeed, a group of three conserved cellular Ser/Thr kinases, the vaccinia
virus-related kinases (VRKs) (21, 22), exhibit similarity (33 to 41% amino acid identity) to
the vaccinia virus B1 kinase (2) and can complement loss of B1 function (15, 23, 24). For
example, seminal studies demonstrated that the expression of VRK1 from the viral
genome can rescue a B1 mutant phenotype (23), paving the way for the discovery that
VRK1 and B1 both regulate BAF. More recently, studies in VRK knockout (KO) cell lines
demonstrated that endogenous VRK2 can complement loss of B1 during ΔB1 virus DNA
replication (15). Importantly, although the replication block resulting from B1 and VRK2
deletion inhibited the vaccinia virus life cycle at the stage of DNA replication, BAF
depletion only modestly rescued ΔB1 virus DNA replication in VRK2 knockout (VRK2KO)
cell lines. We inferred from these data that B1 functioned in an additional, BAF-
independent role to promote vaccinia virus DNA replication (15).

The nature of this additional BAF-independent pathway by which B1 and VRK2
promote vaccinia virus replication was informed by recent findings regarding adap-
tive evolution experiments with ΔB1 vaccinia virus (6). When ΔB1 vaccinia virus was
subjected to iterative passaging, an adapted virus variant emerged that is referred to
herein as ΔB1mutB12. Genome sequencing and functional analysis of this virus mapped
the location of second-site suppressor mutations to insertion/deletion (indel) sites
within the viral *B12R* gene that truncate the B12 protein and result in decreased protein
expression. Intriguingly, B12 is a homolog of B1 and VRK2, with ~34% amino acid
similarity to the vaccinia virus B1 kinase and ~30% amino acid similarity to VRK2 (25).
Unlike B1 and VRK2, B12 possesses substitutions at key residues predicted to be crucial
for phosphotransferase activity in canonical kinases, thereby meeting the definition of
a pseudokinase (25–27). Though pseudokinases may lack enzymatic activity, they are
not functionally inert; pseudokinases are increasingly being identified as major regu-
lators of signal transduction in many species (28, 29). The precise function of vaccinia

virus B12 during infection has remained enigmatic to date. Specifically, previous studies of a B12 deletion mutant, lacking 83% of the *B12R* gene, revealed that this B12 deletion virus replicated efficiently in cultured cells and *in vivo* (26); however, when B12 was deleted in the context of the vaccinia virus B1 deletion mutant ΔB1mutB12, B12 was revealed to be repressive to vaccinia virus replication (6). Considering this evidence that B12 acts as a repressor of vaccinia virus replication upon loss of B1, we sought to determine whether the requirement of vaccinia virus for either vaccinia virus B1 or the cellular kinase VRK2 is functionally linked to vaccinia virus B12.

In this report, we characterize in detail the vaccinia virus replication block resulting from deletion of both B1 and VRK2 and demonstrate that loss of B12 is sufficient to mitigate the B1- and VRK2-dependent block in viral DNA replication. We further demonstrate that B12 colocalizes with VRK2A and VRK2B and copurifies with VRK2A in immunoprecipitation assays. Additionally, insight into the replication block caused by B12 repression revealed that B12's repressive activity coincides with the inability of vaccinia virus replication factories to form. Lastly, we demonstrate that B12 is inhibited by enzymatically active B1 or VRK2A but not by enzymatically active VRK2B or catalytically inert B1, VRK2A, or VRK2B. Together, our studies of B1, VRK2, and B12 present evidence that B12 is capable of repressing vaccinia virus at a prereplicative stage of the vaccinia virus life cycle and lead us to infer that B1 and VRK2A function to inhibit this repressive function of B12 via phosphorylation of either B12 or an unknown substrate.

## RESULTS

**VRK2 is required in HAP1 cells for optimal replication of ΔB1 vaccinia virus but is not necessary for replication of WT vaccinia virus, HSV-1, or Ad5.** Encoding one or more VRK homologs is a unique property of most poxviruses, distinct from other large DNA viruses. For this reason, we hypothesized that other viruses would be dependent on VRK2 for viral replication. To test this hypothesis, a poxvirus (VACV), herpes simplex virus 1 (HSV-1), and adenovirus type 5 (Ad5) were assessed for viral replication in the presence and absence of VRK2 (Fig. 1). Viral DNA accumulation and yield were determined in parental human near-haploid (HAP1) cells and VRK2 knockout HAP1 (VRK2KO) cells infected with either wild-type (WT) or ΔB1 vaccinia virus (Fig. 1A). At 24 h postinfection (hpi), WT vaccinia virus DNA accumulation was unaffected by the deletion of VRK2; however, ΔB1 vaccinia virus DNA accumulation was significantly inhibited by VRK2 deletion (Fig. 1A, left). Specifically, in the parental HAP1 cells, ΔB1 DNA accumulation was similar to that of WT virus, whereas in the VRK2KO cells, ΔB1 DNA accumulation was reduced 29-fold compared to that in ΔB1-infected HAP1 cells (Fig. 1A, left, compare hatched bars). Regarding viral progeny, the WT vaccinia virus titer was unaffected by the deletion of VRK2; however, the ΔB1 vaccinia virus titer was significantly inhibited by VRK2 deletion (Fig. 1A, right). In these experiments, while the viral yield of ΔB1 virus did not reach WT virus levels in the HAP1 cells (53-fold reduction), VRK2 deletion further reduced the ΔB1 viral yield 11-fold compared to the HAP1 cell ΔB1 viral yield (Fig. 1A, right, compare hatched bars), which corresponds to a 548-fold reduction compared to the viral yield of VRK2KO cell WT virus infection. For comparison, the replication of HSV-1 and Ad5 were evaluated in HAP1 and VRK2KO cells as examples of DNA viruses which lack an obvious VRK homolog (Fig. 1B and C). Importantly, although vaccinia virus DNA accumulation and viral yield were affected by VRK2 deletion, the yields of HSV-1 and Ad5 were unaffected by the absence of VRK2. These results demonstrate a specific dependence of vaccinia virus on the cellular kinase VRK2, suggesting that B1 and VRK2 signaling is mediated via a vaccinia virus protein(s) to promote viral replication.

**A ΔB1 virus adaption mutant (ΔB1mutB12) with a truncated B12 pseudokinase is unaffected by VRK2 deletion.** Having established that the requirement for B1 or VRK2 was unique to vaccinia virus, we next posited that the requirement of vaccinia virus for either B1 or VRK2 is dependent on the repressive activity of vaccinia virus B12 (6). To address this hypothesis, we determined whether ΔB1mutB12 virus retained its sensitivity to the absence of VRK2 as observed for the ΔB1 virus. Viral DNA accumula-
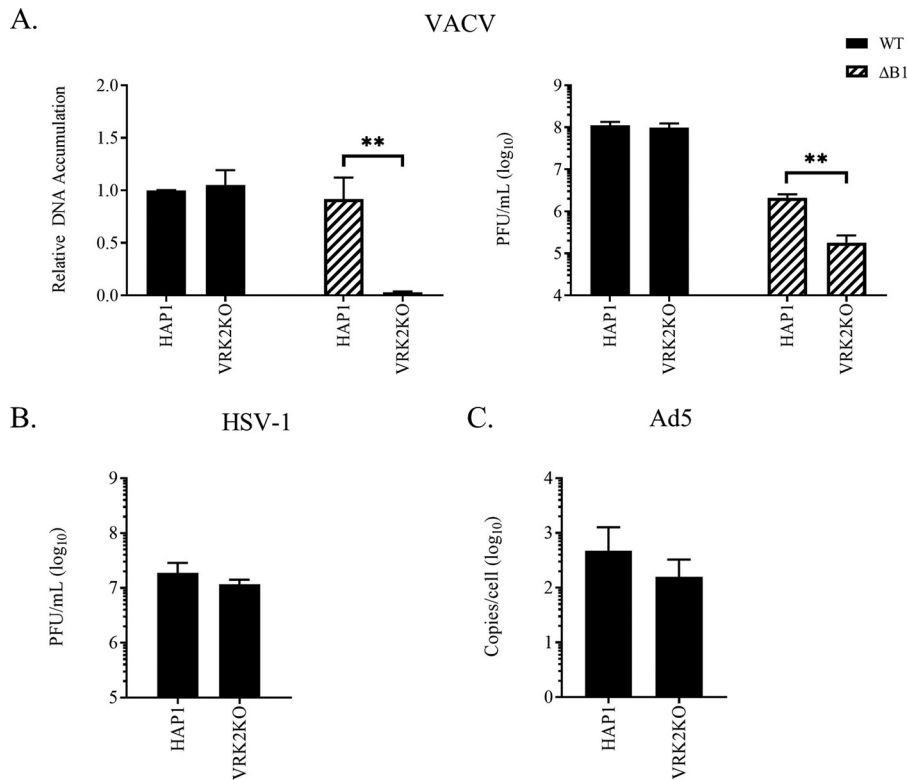
**FIG 1** VRK2 is required for vaccinia virus replication in the absence of B1 but is not required for HSV-1 or Ad5 replication. (A) Vaccinia virus DNA accumulation (left) and viral yield (right) measured for WT or ΔB1 virus at 24 hpi in HAP1 control or VRK2KO cell lines infected at an MOI of 3. (B) HSV-1 viral yield at 72 hpi in HAP1 control or VRK2KO cell lines infected at an MOI of 0.1. (C) Adenovirus DNA accumulation at 48 hpi in HAP1 control or VRK2KO cell lines infected at 500 virus particles per cell. **, $P < 0.01$.

tion and yield were determined in HAP1 and VRK2KO cells infected with either WT, ΔB1, or ΔB1mutB12 vaccinia virus (Fig. 2). At 24 hpi, no difference in virus DNA accumulation was observed for WT virus upon VRK2 deletion (Fig. 2, left). As for Fig. 1, ΔB1 virus DNA accumulation in the VRK2KO cells was reduced 7.8-fold compared to the ΔB1 virus DNA accumulation in HAP1 cells (Fig. 2, left). In contrast, when ΔB1mutB12 virus was assessed in HAP1 and VRK2KO cells at 24 hpi, DNA accumulation was similar in the two cell lines (Fig. 2, left, compare open bars). In terms of viral yield, VRK2 deletion did not affect WT virus, but it decreased the ΔB1 infection titer 7.5-fold compared to the ΔB1 virus titer in HAP1 cells (Fig. 2, right). When viral titers were assessed during ΔB1mutB12
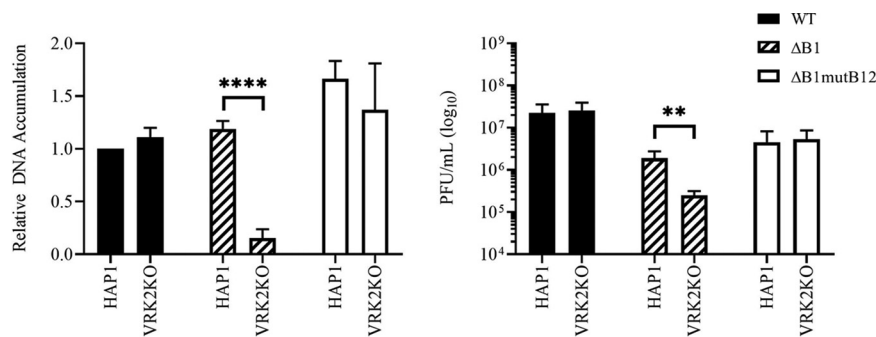


**FIG 2** A ΔB1 virus B12 evolution mutant that has adapted to growth in the absence of B1 no longer requires VRK2 for DNA replication. Vaccinia virus DNA accumulation (left) and viral yield (right) measured for WT, ΔB1, or ΔB1mutB12 virus at 24 hpi in HAP1 control or VRK2KO cell lines infected at an MOI of 3. **, $P < 0.01$; ****, $P < 0.0001$.

virus infection, no differences were observed between the HAP1 and VRK2KO cells (compare open bars) (Fig. 2, right). These data demonstrate that mutation of the B12R gene rescues the block in vaccinia virus DNA replication established by B1 and VRK2 deletion and are consistent with a model in which B1 and VRK2 antagonize B12 via a shared pathway.

**VRK2 is required in primary NHDF cells for optimal replication of ΔB1 vaccinia virus but is not necessary for WT or ΔB1mutB12 virus.** To determine if this putative B1/VRK2/B12 signaling axis is intact in primary cells, we employed small interfering RNA (siRNA)-mediated knockdown of VRK2 in primary human neonatal dermal fibroblast NHDF cells. Using this approach, treatment of NHDF cells with an siRNA targeting VRK2 (siVRK2) resulted in approximately 90% depletion of endogenous VRK2 protein following a 4-day VRK2 depletion (Fig. 3B). Subsequently, viral DNA accumulation and yield were determined in NHDF cells following siVRK2 or control siRNA (siCTRL) treatment (Fig. 3A). At 24 hpi, no difference in virus DNA accumulation was observed for WT virus upon VRK2 depletion in NHDF cells (Fig. 3A, left). ΔB1 virus DNA accumulation in siVRK2-treated NHDF cells was reduced 7.3- or 5.5-fold compared to its accumulation in the untreated or siCTRL-treated control, respectively (Fig. 3A, left, compare hatched bars). Conversely, ΔB1mutB12 vaccinia virus DNA accumulation in NHDF cells was not affected by the depletion of VRK2 (Fig. 3A, left, compare open bars). Regarding viral yields, we saw trends similar to those in our DNA accumulation studies, with VRK2 depletion only affecting ΔB1 virus (Fig. 3A, right, compare hatched bars). These data demonstrate that reduced B12 expression rescues the block in vaccinia virus DNA replication established by B1 deletion and VRK2 depletion. Accordingly, we conclude that B1 and VRK2 antagonize B12 in a primary cell line, as well as in HAP1 cells.

To further investigate vaccinia virus replication in the NHDF cells, representative viral early and late protein expression were assessed during infection (Fig. 3C). Early protein expression, measured by viral I3 expression at 7 hpi, was present at equivalent levels during WT, ΔB1, and ΔB1mutB12 infection regardless of siRNA treatment (Fig. 3C). However, late protein expression, measured by viral F17 (also referred to as F18 in the literature) expression at 24 hpi, was virus and siRNA dependent (Fig. 3C). WT infections of untreated, siCTRL-, or siVRK2-treated NHDF cells all resulted in robust F17 protein expression. In contrast, ΔB1 infections resulted in lower levels of F17 expression, and the expression varied by siRNA treatment. While ΔB1 infections of untreated or siCTRL-treated NHDF cells both resulted in detectable F17 expression, ΔB1 infection of siVRK2-treated NHDF resulted in undetectable expression of F17. Lastly, ΔB1mutB12 infections of untreated, siCTRL-, or siVRK2-treated NHDF cells all resulted in similar levels of F17 expression among siRNA treatments, though F17 expression during ΔB1mutB12 infections was lower than that of WT virus infection and higher than that of ΔB1 virus infection. Next, late protein expression was assayed through detection of mCherry protein regulated by a late viral promoter at 24 hpi (Fig. 3D). mCherry protein expression followed a trend similar to that observed for F17 protein expression. During ΔB1 virus infections of untreated or siCTRL-treated NHDF cells, mCherry was clearly expressed; however, ΔB1 virus infection of siVRK2-treated NHDF cells resulted in undetectable mCherry expression. In contrast, ΔB1mutB12 infections of NHDF cells exhibited no difference in mCherry expression between siCTRL and siVRK2 treatments. These data agree with the studies of HAP1/VRK2KO cells and support the idea that, in a primary cell line, B1 and VRK2 both promote vaccinia virus infection by acting in part to inhibit the repressive activity of vaccinia virus B12.

**B1 and VRK2 interact with B12 in uninfected and infected cells.** Having demonstrated that loss of B12 rescues ΔB1 virus replication in cells lacking VRK2, we investigated whether interaction between B1 or VRK2 and B12 could be detected either through immunofluorescence analysis of fixed cells or by protein immunoprecipitation. Previous studies have determined that B1 and B12 do not overtly colocalize, since B12 is expressly nuclear in its localization, whereas B1 is diffusely localized to the cytoplasm in the absence of infection and localizes to vaccinia virus replication factories during
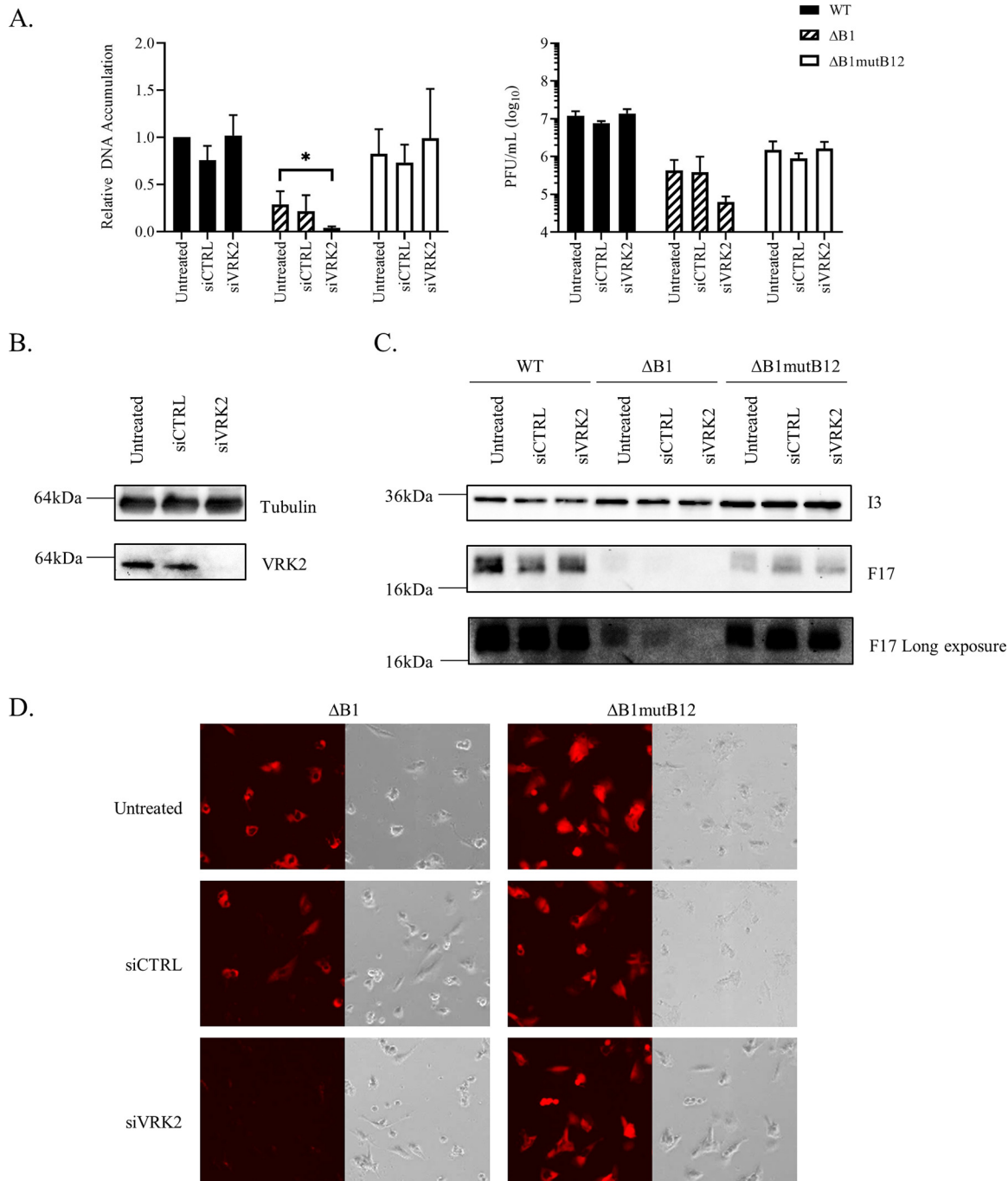
FIG 3 VRK2 or B1 is required to inhibit B12 and promote vaccinia virus replication in multiple cell lines. Primary NHDF cells were treated with siRNA and infected with WT, ΔB1, or ΔB1mutB12 virus 3 days postdepletion at an MOI of 3. (A) Vaccinia virus DNA accumulation (left) and viral yield (right) measured for WT, ΔB1, or ΔB1mutB12 virus at 24 hpi in NHDF cells depleted of VRK2. (B) Protein immunoblotting of tubulin and VRK2 in uninfected cells harvested 3 days after siRNA treatment. (C) Protein immunoblotting of I3, a vaccinia virus early protein, at 7 hpi and of F17, a vaccinia virus late protein, at 24 hpi in NHDF cells depleted of VRK2 and then infected with WT, ΔB1, or ΔB1mutB12 virus. (D) mCherry fluorescence of ΔB1 or ΔB1mutB12 virus at 24 hpi in NHDF cells depleted of VRK2. *, $P < 0.05$.

infection (6, 15). However, B12 colocalization with VRK2 has not yet been assessed. Previous studies have demonstrated that VRK2 is expressed as two isoforms, VRK2A and VRK2B, with divergent localizations (22, 30). VRK2A is the larger isoform, as it contains a transmembrane domain at its C terminus that results in membrane localization, whereas VRK2B is truncated via alternative splicing and does not contain a transmembrane domain, resulting in diffuse localization to both the nucleus and cytoplasm. To

A.



B.
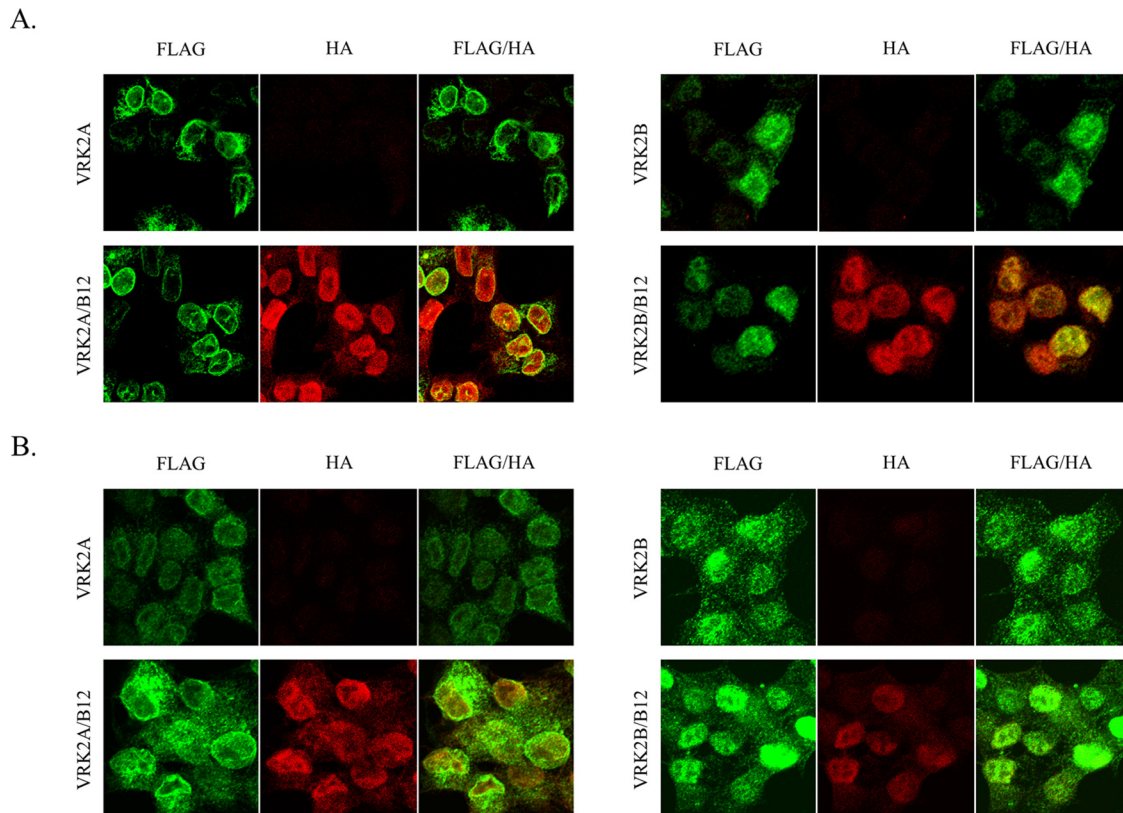


**FIG 4** VRK2A, VRK2B, and B12 colocalize in VRK2KO cells. 3×FLAG-tagged VRK2A or VRK2B with or without HA-tagged B12 was overexpressed in VRK2KO cells by lentiviral transduction, and following selection, cells were seeded on poly-L-lysine-coated slides, fixed, permeabilized, and stained with rabbit anti-FLAG and mouse anti-HA antibodies. (A) Immunofluorescence analysis of cells for localization of VRK2A or VRK2B (green) when expressed alone (top) or when expressed in the presence of B12 (red) (bottom) in uninfected cells. (B) Immunofluorescence analysis of cells for localization of VRK2A or VRK2B (green) when expressed alone (top) or in the presence of B12 (red) (bottom) during WRHAB12 vaccinia virus infection (6 hpi, MOI of 5).

examine the localization of VRK2 and B12 in uninfected cells, 3×FLAG-tagged VRK2A (3XFLAGVRK2A) and 3XFLAGVRK2B were stably expressed in VRK2KO cells with or without hemagglutinin (HA)-tagged B12. Each construct contained a FLAG or HA epitope tag at its N terminus and was expressed using a lentiviral expression system conveying either hygromycin (FLAG-tagged VRK2) or puromycin (HA-tagged B12) resistance. The truncated alternate splice variant of VRK2, VRK2B, was generated by altering the VRK2A reading frame starting at amino acid 395 to GRSLGY followed by a stop codon, as occurs in VRK2B.

When expressed individually in uninfected cells, VRK2A and VRK2B localized as previously reported (Fig. 4A, top). VRK2A's localization was consistent with expression in the membrane of the endoplasmic reticulum (ER) and nucleus, whereas VRK2B localized diffusely throughout the cytoplasm and nucleus. When VRK2A and VRK2B were expressed in conjunction with B12 in uninfected cells (Fig. 4A, bottom panels), we did not observe any alteration of localization for either VRK2 protein (Fig. 4A, compare top and bottom images for each of VRK2A and VRK2B); however, we did observe that the localization of VRK2A and VRK2B overlapped with that of B12. Finally, we assayed VRK2's colocalization with B12 during vaccinia virus infection. For these studies, cells were transduced with 3XFLAGVRK2A or 3XFLAGVRK2B and then infected with a recombinant vaccinia virus (WR strain) that expresses HA-tagged B12 (HAB12) from its thymidine kinase locus, WRHAB12 (6). When the localization of VRK2A, VRK2B, and B12 was assessed during WRHAB12 vaccinia virus infection, we saw results similar to those in uninfected cells (Fig. 4B). Together, these studies provide evidence that both isoforms of VRK2 colocalize with B12 in uninfected and infected cells.
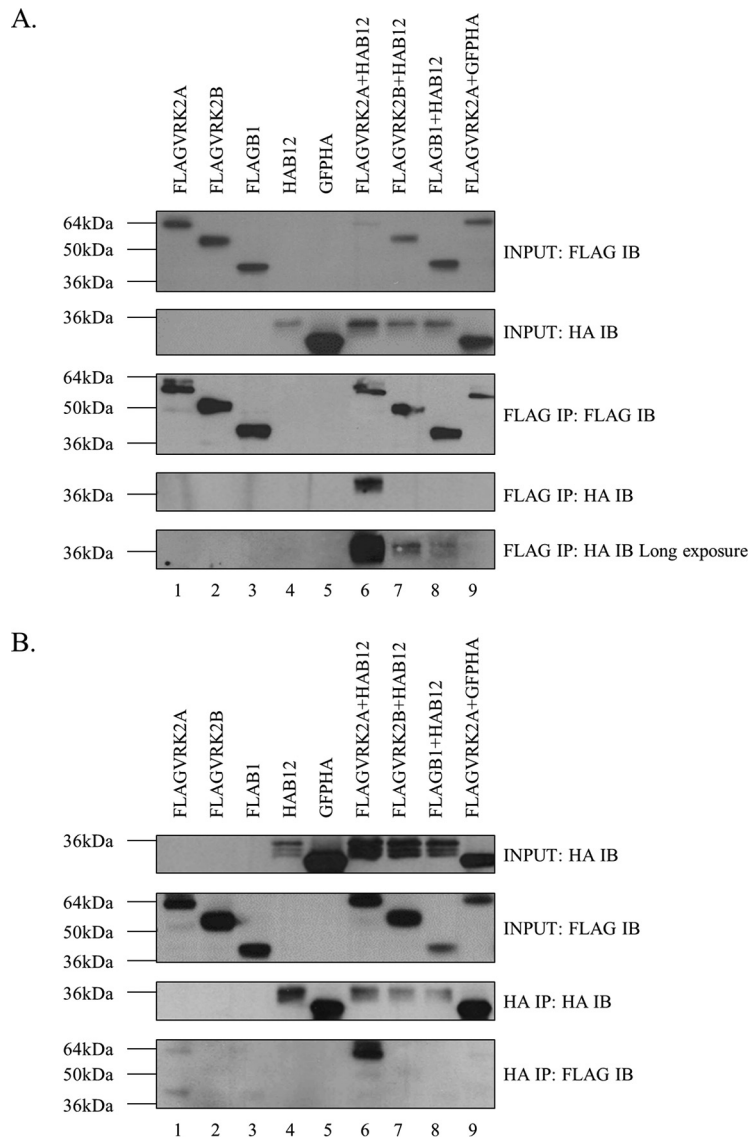
**FIG 5** VRK2A interacts with B12 in uninfected VRK2KO cells. 3×FLAG-tagged VRK2A, VRK2B, or B1 and HA-tagged B12 or GFP were overexpressed alone or tandem in VRK2KO cells by lentiviral transduction. (A and B) Following selection, cell lysates were collected and subjected to immunoprecipitation (IP) using anti-FLAG or anti-HA antibody magnetic beads, followed by protein immunoblotting (IB) of FLAG and HA. Input lysates were included to illustrate the presence of the respective tagged proteins in each lysate. (A) FLAG IP. (B) HA IP.

Next, we assessed whether B12 copurified with B1 or either VRK2 protein after immunoprecipitation from uninfected or infected cells. For immunoprecipitations of uninfected cells, the respective construct(s) were stably expressed in VRK2KO cells using lentiviral expression system(s) and antibiotic selection. Immunoblots of input lysates were performed to verify expression of the respective 3×FLAG- or HA-tagged proteins (Fig. 5A and B, INPUT). The same lysates were subjected to immunoprecipitation using anti-FLAG magnetic beads and subsequent immunoblot analysis with HA-specific antibody to determine whether HAB12 was coprecipitated with the FLAG-tagged proteins (Fig. 5A, IP and IB). We found that 3XFLAGVRK2A coprecipitated with HAB12 but not the HA-tagged-green fluorescent protein (GFP) control construct (GFPHA) (Fig. 5A, FLAG IP: HA IB, compare lanes 6 and 9). HAB12 also coprecipitated with the 3XFLAGVRK2B isoform, although it is noteworthy that 3XFLAGVRK2B copurified HAB12 at a much lower level than did 3XFLAGVRK2A (Fig. 5A, FLAG IP: HA IB,

A.



B.



C.
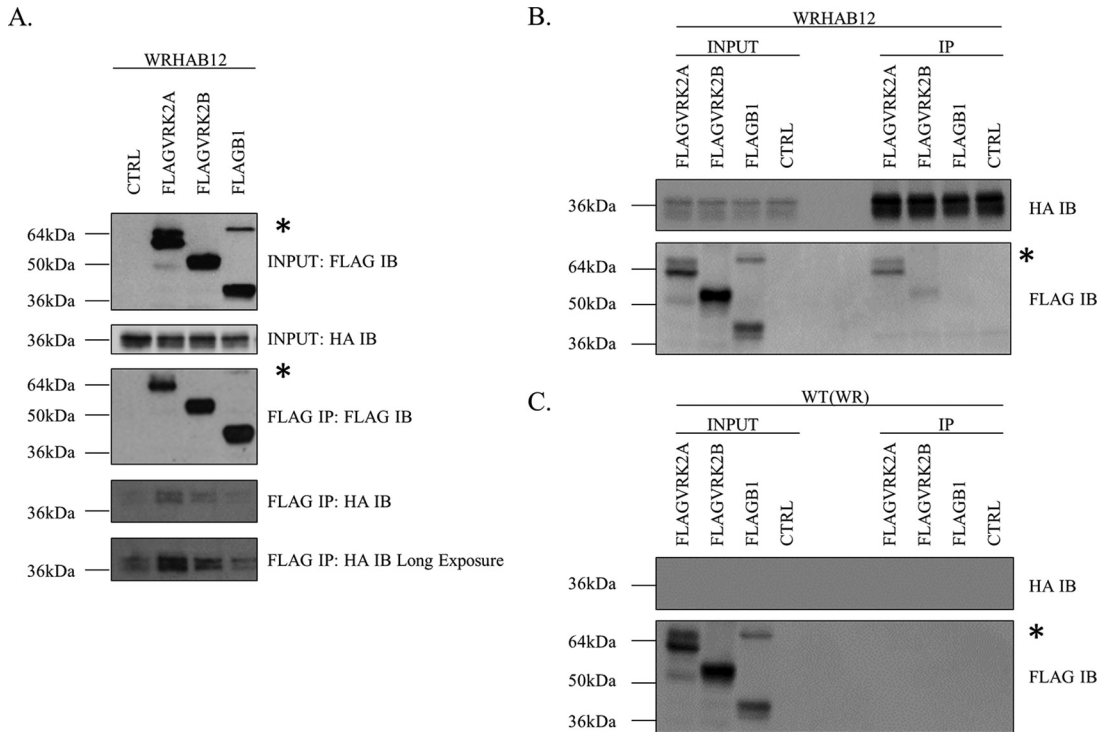


**FIG 6** VRK2A interacts with B12 in infected VRK2KO cells. 3×FLAG-tagged VRK2A, VRK2B, or B1 was overexpressed in VRK2KO cells by lentiviral transduction. (A) Following selection, cells were infected with WRHAB12 or wild-type WR virus at an MOI of 5. At 7 hpi, cell lysates were subjected to immunoprecipitation using anti-FLAG or anti-HA antibody magnetic beads, followed by protein immunoblotting of FLAG and HA. Input lysates were included to illustrate the presence of the respective tagged proteins in each lysate. The asterisks indicate oligomerized 3×FLAG-tagged B1. (A) WRHAB12 virus infection; anti-FLAG antibody IP. (B) WRHAB12 virus infection; anti-HA antibody IP. (C) WR virus infection; anti-HA antibody IP.

compare lanes 6 and 7). Lastly, we found that 3XFLAGB1 also retrieved HAB12, again at a lower efficiency than 3XFLAGVRK2A (Fig. 5A, FLAG IP: HA IB, compare lanes 6 and 8). To complement these studies, we next examined the ability of HAB12 to coprecipitate FLAG-tagged B1, VRK2A, or VRK2B using anti-HA antibody magnetic beads (Fig. 5B). We found that HAB12 coprecipitated 3XFLAGVRK2A (Fig. 5B, HA IP: FLAG IB, compare lanes 6 and 9); however, we were unable to corroborate the interaction between HAB12 and 3XFLAGVRK2B or 3XFLAGB1 using reciprocal immunoprecipitation (Fig. 5B, HA IP: FLAG IB, lanes 7 and 8).

For immunoprecipitations of HAB12 in infected cells, cells were transduced with 3XFLAGB1, 3XFLAGVRK2A, or 3XFLAGVRK2B and then infected with WRHAB12 or wild-type (WR) virus. Immunoblots of lysates verified the expression of the respective 3×FLAG- or HA-tagged proteins (Fig. 6A, INPUT). The same lysates were subjected to immunoprecipitation using anti-FLAG antibody magnetic beads and subsequent immunoblot analysis with HA-specific antibody to determine whether HAB12 was coprecipitated with the FLAG-tagged proteins in WRHAB12-infected cells. We found that 3XFLAGVRK2A efficiently coprecipitated HAB12 and 3XFLAGVRK2B weakly coprecipitated HAB12 (Fig. 6A, FLAG IP: HA IB). However, during WRHAB12 infection, 3XFLAGB1 did not coprecipitate HAB12 above background levels. To complement these studies, we next examined the ability of HAB12 to coprecipitate FLAG-tagged B1, VRK2A, or VRK2B during WRHAB12 infection using anti-HA antibody magnetic beads (Fig. 6B). We found that HAB12 coprecipitated 3XFLAGVRK2A most effectively but additionally coprecipitated detectable levels of 3XFLAGVRK2B. As we observed nonspecific pulldown of 3×FLAG-tagged proteins by the anti-HA antibody magnetic beads during uninfected-cell-lysate immunoprecipitations (Fig. 5B), we simultaneously performed HA immunoprecipitations during wild-type WR infection as a negative control (Fig. 6C). In the absence of HAB12, neither 3XFLAGVRK2A nor 3XFLAGVRK2B coprecipitated with
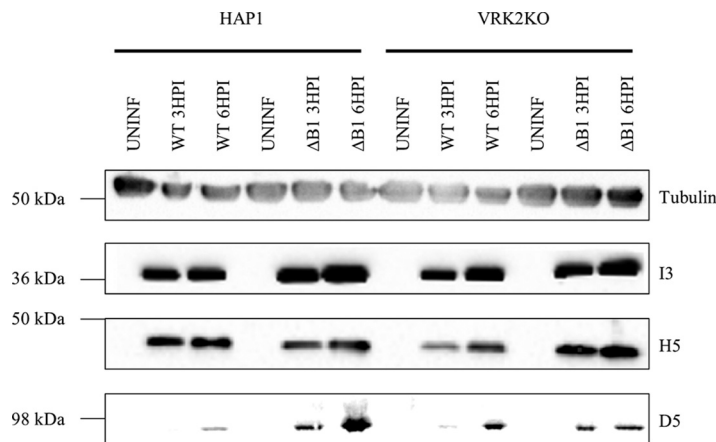
**FIG 7** B12 does not inhibit the expression of the respective vaccinia virus early proteins in the absence of B1 and VRK2. Protein immunoblotting of tubulin, I3, H5, and D5 in HAP1 or VRK2KO cells following WT or ΔB1 vaccinia virus infection at 3 or 6 hpi at an MOI of 10. UNINF, uninfected cells.

the anti-HA antibody magnetic beads. Considered together, we infer from these data that the VRK2A and B12 proteins interact either directly or via a larger complex containing both VRK2A and B12. Additionally, we demonstrate that VRK2B and B1 also interact with B12, albeit more weakly. Interestingly, despite the near identity of VRK2A and VRK2B, striking differences in interaction with B12 were observed, highlighting a key variation in VRK2A and VRK2B properties.

**Early protein expression is unaltered by VRK2 deletion.** Having established that B12 is necessary for the suppression of ΔB1 virus DNA replication in VRK2KO cells, we sought to better define the execution point of the viral life cycle at which B12 was acting. We therefore assessed early events in vaccinia virus replication for B1 and VRK2 dependence in the presence of B12, including early protein expression. If B12 impedes vaccinia virus via inhibition of viral early protein expression, we posited that a subset or all vaccinia virus early proteins would be absent during infections repressed by B12. Thus, the abundance of viral proteins early in expression was measured in HAP1 and VRK2KO cells infected with either WT or ΔB1 virus using two complementary approaches.

First, examination of early protein expression by immunoblotting of three representative viral proteins (I3, D5, and H5) revealed that no significant differences were observed in the levels of these proteins either in HAP1 cells infected with WT or ΔB1 virus or in VRK2KO cells infected with WT virus compared to the levels in VRK2KO cells infected with ΔB1 virus (Fig. 7). Interestingly, D5 was modestly increased in abundance during ΔB1 virus infection compared to its levels in WT virus infection. For a more comprehensive analysis of the viral proteome in the early stages of infection, HAP1 or VRK2KO cells were infected with WT or ΔB1 virus for 7 h prior to collection of protein lysates for mass spectrometry analysis. Total protein samples from infected whole-cell lysates were precipitated, digested with trypsin, and analyzed by liquid chromatography-tandem mass spectrometry (LC-MS/MS). The Scaffold software package facilitated the analysis of thousands of high-confidence peptide identifications, which were then used to determine whether a protein was expressed at a detectable level based on a two-peptide cutoff. Overall, as compared to the vaccinia virus and cellular proteomes, 134 viral and ~2,200 cellular proteins were identified as "expressed" based on this cutoff. The vaccinia virus proteins identified were then compared to the complete vaccinia virus proteome and used to assess the presence or absence of each respective protein. To examine protein expression by temporal expression class, the vaccinia virus proteome was subcategorized into early, intermediate, or late protein expression using transcriptome profiling from Yang et al. (31). Ten gene products from the vaccinia virus WR reference proteome that were not characterized by Yang et al. were removed from
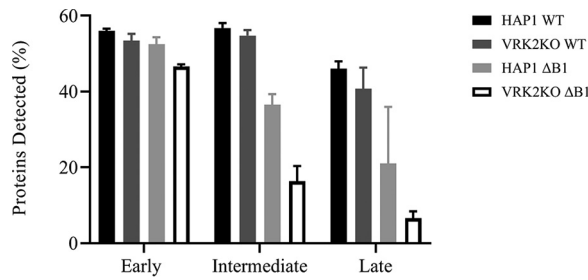
**FIG 8** B12 does not inhibit vaccinia virus early protein expression in the absence of B1 and VRK2. HAP1 or VRK2KO cells were infected with WT or ΔB1 vaccinia virus at 7 hpi at an MOI of 10. Cell lysates were then collected and subjected to proteomics analysis for vaccinia virus proteins. Bar graphs represent the percentage of each vaccinia virus gene class detected by sample.

the expression class analysis, refining the proteome used as a reference in our analysis to 207 potential proteins with 117, 52, and 38 proteins expressed at early, intermediate, and late times, respectively.

Proteomics analysis revealed clear contrasts in the percentages of vaccinia virus proteins detected after ΔB1 virus infections of VRK2KO cells in comparison to the percentages in all other groups, with the most striking differences in the intermediate and late temporal classes (Fig. 8). Specifically, for ΔB1 virus-infected VRK2KO cell lysates, 47% of early, 16% of intermediate, and 7% of late vaccinia virus proteins were expressed as determined by mass spectrometry. In comparison, WT virus infection of HAP1 cells resulted in 56%, 57%, and 46% expression of each respective temporal class. WT virus infection of VRK2KO cells resulted in 53%, 55%, and 41% expression of each respective temporal class. Lastly, ΔB1 virus infection of HAP1 cells resulted in 53%, 37%, and 21% expression of each respective temporal class. Importantly, early protein expression levels remained relatively constant at 56%, 53%, 53%, and 47% expression between WT virus infection of HAP1 cells, WT virus infection of VRK2KO cells, ΔB1 virus infection of HAP1 cells, and ΔB1 virus infection of VRK2KO cells, respectively. The resulting expression pattern is indicative of ΔB1 virus infection of VRK2KO cells proceeding through early protein expression with an efficiency similar to those of the other virus and cell combinations. When examined more closely (Table 1; see the supplemental material), the abundance of early proteins (measured by the total number of spectra identified for a protein) shows a bias toward higher abundance during ΔB1 virus infection of VRK2KO cells compared to their abundances in other groups. These data argue against defective early protein expression during ΔB1 virus infection of VRK2KO cells and instead are consistent with prior studies which demonstrated increased early protein expression as a result of impaired DNA replication (32). Together,

**TABLE 1** Average total spectrum counts for proteomic analysis of whole-cell lysates of infected cells

| Function | Gene | Time of expression | Avg no. of total spectra (total spectrum counts of replicate experiments [n = 2]) | | | |
|---|---|---|---|---|---|---|
| | | | HAP1 WT | HAP1 ΔB1 | VRK2KO WT | VRK2KO ΔB1 |
| DNA polymerase | E9 | Early | 24.5 (37, 12) | 44 (65, 23) | 22 (28, 16) | 41.5 (58, 25) |
| Primase/helicase | D5 | Early | 19.5 (24, 15) | 24.5 (29, 20) | 16 (19, 13) | 22.5 (27, 18) |
| Protein kinase | B1 | Early | 12.5 (12, 13) | ND[a] | 11 (10, 12) | ND |
| Processivity factor | A20 | Early | 2 (0, 4) | 4.5 (3, 6) | 2.5 (2, 3) | 4 (3, 5) |
| Uracil DNA glycosylase | D4 | Early | ND | 3 (4, 2) | ND | 1 (ND, 2) |
| ssDNA binding | I3 | Early | 61.5 (61, 62) | 98.5 (112, 85) | 62 (69, 55) | 101.5 (136, 67) |
| Scaffolding protein | H5 | Early | 98 (88, 108) | 190.5 (240, 141) | 91.5 (77, 106) | 177 (237, 117) |
| Telomere binding | I1 | Intermediate | 92 (89, 95) | 38.5 (43, 34) | 96.5 (96, 97) | 11.5 (15, 8) |
| Viral membrane formation | A6 | Intermediate | 40.5 (39, 42) | 8.5 (9, 8) | 46 (50, 42) | ND |
| Virion membrane biogenesis | A11 | Late | 18.5 (19, 18) | 1 (0, 2) | 16.5 (16, 17) | ND |
| LB phosphoprotein | F17 | Late | 17.5 (19, 16) | 16.5 (27, 6) | 17 (19, 15) | 6.5 (10, 3) |

[a]ND, not detected.
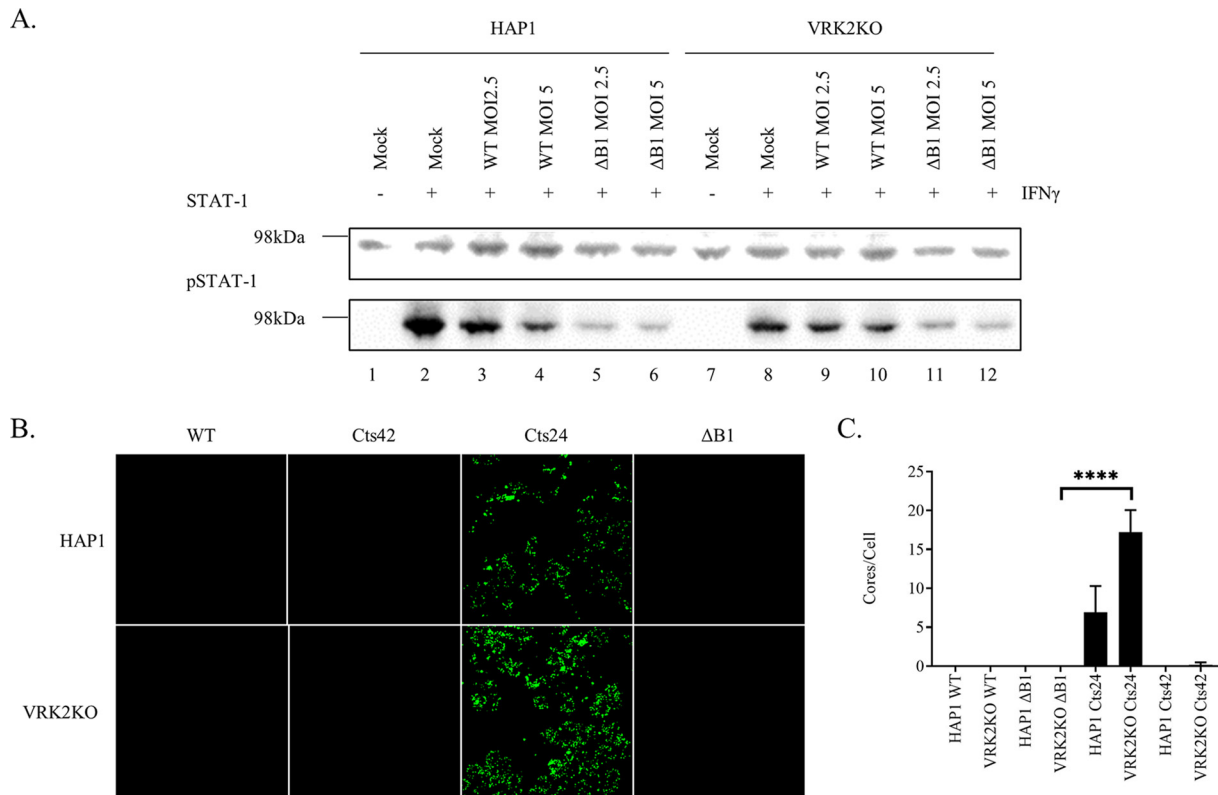
**FIG 9** VRK2 and B1 do not function to inhibit B12 repression of vaccinia virus uncoating. (A) STAT-1 dephosphorylation following vaccinia virus infection. Representative STAT-1 immunoblot analysis of cell lysates from HAP1 or VRK2KO cells following WT or ΔB1 vaccinia virus infection for 1 h and IFN-γ treatment for 0.5 h after the 1-h infection. (B and C) Immunofluorescence of vaccinia viral cores following infection. (B) Representative images of immunofluorescence in infected HAP1 control and VRK2KO cells. Cells were infected with WT, ΔB1, Cts42, or Cts24 virus at an MOI of 5 for 4 h at 39.7°C. (C) Intact (not uncoated) viral cores per cell were quantified with ImageJ software ($n = 3$). ****, $P < 0.0001$.

these data lead to the conclusion that ΔB1 virus infection of VRK2KO cells is not restricted at the point of early protein expression.

**ΔB1 virus uncoating is unaffected by B12 expression.** To assess whether the observed DNA replication block was due to a B12 execution point at this stage in the viral life cycle, two distinct approaches were used to examine virion uncoating during ΔB1 virus infection of VRK2KO cells. We posited that if B12 were repressing vaccinia virus uncoating, ΔB1 virus infection of VRK2KO cells would be arrested at this stage, while all other infections would proceed through this stage. Vaccinia virus uncoating was measured using both a STAT-1 dephosphorylation-based core activation assay (33) and an immunofluorescence-based A4 core dissolution assay (34).

First, we monitored STAT-1 dephosphorylation as a measure of viral core activation (33). It has been shown previously that the viral H1 phosphatase associated with incoming virus catalyzes the dephosphorylation of STAT-1, blocking its phosphorylation in response to gamma interferon (IFN-γ) (33). Importantly, for H1 to dephosphorylate STAT-1, it must be liberated from the lateral bodies of the core during the first step of vaccinia virus uncoating, core activation. Using STAT-1 dephosphorylation after IFN-γ treatment as a proxy for lateral body disassembly, core activation following ΔB1 virus infection of VRK2KO cells was determined (Fig. 9A). Treatment of uninfected HAP1 and VRK2KO cells with IFN-γ for 0.5 h results in rapid phosphorylation of STAT-1 compared to its phosphorylation in uninduced cells (Fig. 9A, compare lanes 1 with 2 and 7 with 8). Infection of HAP1 cells with WT virus for 1 h prior to IFN-γ treatment reduced STAT-1 phosphorylation compared to its phosphorylation in uninfected IFN-γ-treated cells (Fig. 9A, compare lanes 3 and 4 with 2). Similarly, WT infection of VRK2KO cells prior to IFN-γ treatment reduced phosphorylated STAT-1 levels compared to the phosphorylation of

uninfected induced cells (Fig. 9A, compare lanes 9 and 10 with 8). ΔB1 virus infection of HAP1 cells prior to IFN-γ treatment reduced phosphorylated STAT-1 levels compared to the levels in uninfected induced cells (Fig. 9A, compare lanes 5 and 6 with 2). Lastly, during vaccinia virus infections lacking both B1 and VRK2 (ΔB1 virus infection of VRK2KO cells), STAT-1 phosphorylation is reduced compared to its phosphorylation in uninfected induced cells (Fig. 9A, compare lanes 11 and 12 to 8). Using STAT-1 dephosphorylation as an indicator of lateral body disassembly and core activation, we observed no evidence of aberrant uncoating in VRK2KO cells infected with ΔB1 virus, indicating that ΔB1 infection proceeds normally through this stage in the viral life cycle.

We next addressed whether core dissolution is repressed by B12 during ΔB1 virus infection of VRK2KO cells. To assess core dissolution, we quantified intact viral cores using antibody to the A4 core protein (34). This microscopy-based assay relies on the fact that viral cores are destabilized during uncoating and their presence or absence can be detected by immunostaining as a gauge of uncoating (34, 35). In the absence of uncoating, A4 remains associated with intact viral cores and discrete puncta can be seen after staining. However, after uncoating has occurred, A4 is no longer associated with intact viral cores and is instead dispersed throughout the cytoplasm, resulting in the absence of puncta. At 4 hpi, HAP1 or VRK2KO cells were fixed and stained with antibody specific to the A4 protein (Fig. 9B and C). Following WT virus infection of HAP1 or VRK2KO cells, A4 staining was absent. Likewise, following infection of HAP1 or VRK2KO cells with E9-deficient Cts42 virus (12), which does not impact uncoating but affects DNA replication, staining was absent. Conversely, when HAP1 or VRK2KO cells were infected with D5-deficient Cts24 virus, which has an uncoating-deficient phenotype (36), A4 staining, indicative of intact viral cores, was observed. Finally, when ΔB1 virus infections were performed in both HAP1 and VRK2KO cells, we observed an absence of A4 staining. Collectively, the results of these two uncoating assays suggest that, following entry of ΔB1 virus into VRK2KO cells, the infection progresses normally through uncoating, leading us to conclude that B12 is not impairing events needed for this stage of the virus life cycle.

**Viral replication factory formation is impeded during ΔB1 virus infection of VRK2KO cells.** As ΔB1 virus infection of VRK2KO cells progressed normally through all stages of the vaccinia viral life cycle prior to DNA replication, we next sought to examine viral DNA replication in the absence of B1 and VRK2 in more depth than previously reported. In this effort, viral replication factory formation was measured using an immunofluorescence-based localization assay of the viral I3 single-stranded DNA (ssDNA) binding protein. Following the release of viral genomes into the cytoplasm, vaccinia virus genomic DNA accumulates in cytoplasmic replication factories where DNA replication occurs. In the absence of replication factory formation, I3 is dispersed throughout the cytoplasm. During replication factory formation, I3 localizes to vaccinia virus genomic DNA and forms discrete puncta, which can be made visible by immunofluorescence and that mark the locations of replication factories.

Viral replication factory formation was measured during ΔB1 virus infection of VRK2KO cells to determine if B12 restriction could be observed in the earliest stages of DNA replication. At 4 or 7 hpi, HAP1 or VRK2KO cells were fixed and stained with antibody specific for I3 protein. Following WT virus infection of HAP1 or VRK2KO cells, large, I3-positive replication factories were already present at 4 hpi (Fig. 10A). In comparison, infection of HAP1 or VRK2KO cells with the E9-deficient Cts42 virus, which exhibits a severe defect in DNA replication, also showed the presence of visible puncta by I3 fluorescence (Fig. 10A). However, relative to WT factories, the Cts42 puncta are markedly smaller and likely indicative of input genomes that have completed the uncoating process but have been unable to replicate due to the E9 mutation. Considering another viral mutant, when HAP1 or VRK2KO cells were infected for 4 h with the D5-deficient Cts24 virus, which has an uncoating null phenotype, I3 staining remained diffuse, consistent with a block at the earliest stage of replication factory formation (Fig. 10A). Interestingly, when ΔB1 virus infections were performed in both HAP1 and VRK2KO cells, two different phenotypes were observed at 4 hpi. In the HAP1 cells, the
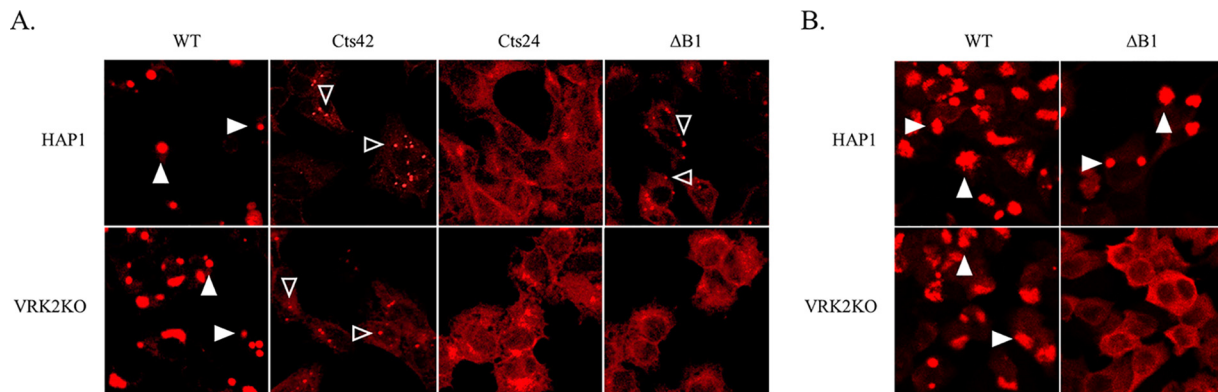
**FIG 10** VRK2KO impedes ΔB1 virus replication factory formation. I3 immunofluorescence analysis of infected HAP1 control and VRK2KO cells. Cells were infected with WT, ΔB1, Cts42, or Cts24 virus at an MOI of 5 at 39.7°C. Replication factory formation was measured at 4 h (A) and 7 h (B). Closed arrowheads indicate replicating vaccinia virus viral factories. Open arrowheads indicate nonreplicating vaccinia virus viral factories.

I3 staining resembled that of the DNA replication null virus, Cts42 (Fig. 10A). These results agree with previously published data (15) showing that ΔB1 virus DNA replication is delayed in HAP1 cells. Strikingly, in the VRK2KO cells, the I3 staining resembled that of the uncoating null virus, Cts24 (Fig. 10A), for which no puncta were observed. We additionally performed the immunofluorescence-based I3 localization assay at 7 hpi with WT and ΔB1 virus (Fig. 10B). At 7 hpi, WT virus infection of HAP1 and VRK2KO cells again resulted in large replication factories. At 7 hpi, ΔB1 virus infection resulted in large replication factories in the HAP1 cells, in agreement with DNA accumulation assay results acquired with quantitative PCR (qPCR) (Fig. 1A and 2). However, in the VRK2KO cells, ΔB1 virus infection continued to result in exclusively diffuse I3 staining even at 7 hpi. These results indicate that though ΔB1 virus infection of VRK2KO cells progressed through all stages of uncoating as determined by STAT-1 dephosphorylation and A4 immunofluorescence, the presence of B12 impedes the ability of vaccinia virus to form replication factories when B1 and VRK2 are absent.

**Enzymatically active VRK2A rescues ΔB1 virus DNA replication and yield in VRK2KO cells.** Since protein kinases have been demonstrated to function both dependently and independently of their catalytic activity, structure/function analysis was used to determine which aspects of VRK2 are required for it to inhibit B12, using cells stably expressing VRK2 variants. For these studies, 1×FLAG-tagged, enzymatically active and catalytically inert VRK2A and VRK2B were stably expressed in VRK2KO cells (Fig. 11A and B). Catalytically inert mutants were generated by introducing a single amino acid change within both the ATP binding and active site in the kinase catalytic domain. Following transduction and hygromycin selection, the expression of each VRK2 variant was confirmed by immunoblot analysis with VRK2 antibody. Regardless of the VRK2 variant, exogenous VRK2 expression in the VRK2KO cell lines modestly exceeded endogenous VRK2A expression in the HAP1 cells (Fig. 11B). Endogenous VRK2B was below the level of detection in parental HAP1 cell lines. (Fig. 11B). Enzymatically active and catalytically inert constructs for both VRK2A (58 kDa) and VRK2B (45 kDa) were expressed at comparable levels (Fig. 11B).

Next, viral DNA accumulation and yield were determined in parental HAP1 and VRK2KO cells stably expressing VRK2 and infected with either WT or ΔB1 vaccinia virus (Fig. 11D). At 24 hpi, WT vaccinia virus DNA accumulation was unaffected by VRK2 deletion or exogenous overexpression (Fig. 11D, left). In contrast, we observed a significant (62-fold) inhibition of ΔB1 virus DNA accumulation upon VRK2 deletion, indicative of repressive activity of B12 (Fig. 11D, left). Only enzymatically active VRK2A was able to substantially rescue ΔB1 virus DNA accumulation, reaching to within 1.2-fold of the accumulation in ΔB1 virus-infected HAP1 cells, whereas enzymatically active VRK2B, catalytically inert VRK2A, and catalytically inert VRK2B failed to contribute significantly to ΔB1 virus DNA accumulation in the VRK2KO cells (24-, 48-, and 41-fold
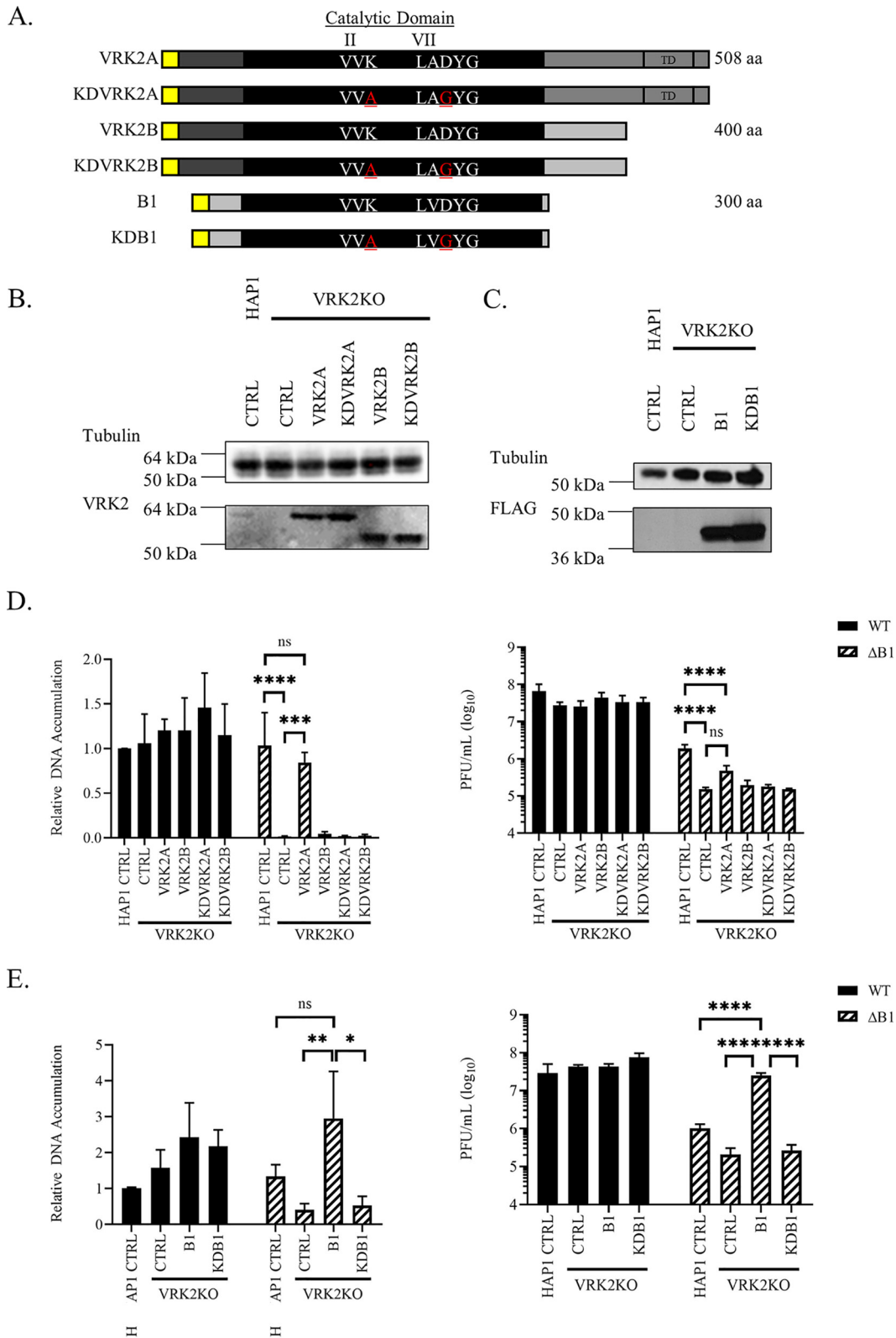
FIG 11 Catalytically active VRK2A and B1 repress B12 inhibitory activity during ΔB1 virus infection. (A) Schematic of 1×FLAG-tagged VRK2A, VRK2B, and B1 kinase constructs. The kinase catalytic domain (black) is conserved throughout the family. Mutations in catalytic domains II (K61A) and VII (D186G) to inactivate kinase activity are in indicated in underlined red. TD, transmembrane domain; yellow, 1×FLAG tag. (B) 1×FLAG-tagged VRK2 was overexpressed in VRK2KO cells by lentiviral transduction followed by selection. VRK2 and tubulin immunoblot analysis of transduced cell lysates for detection of exogenous FLAG-tagged VRK2 protein is shown. (C) 1×FLAG-tagged B1 was overexpressed in VRK2KO cells by lentiviral

(Continued on next page)

reduction, respectively, compared to the ΔB1 virus DNA accumulation in HAP1 cells). The WT viral yield mirrored the WT virus DNA accumulation results and was unaffected by VRK2 deletion or exogenous overexpression of either isoform (Fig. 11D, right). The effect of VRK2 deletion and exogenous overexpression on the ΔB1 virus yield resembled that of ΔB1 virus DNA accumulation in each cell line, though VRK2A exogenous overexpression did not rescue viral yield to the degree that it rescued DNA replication, perhaps due to the inability of VRK2 to complement B1 during later stages of vaccinia virus replication (Fig. 11D, right). At 24 hpi, VRK2 deletion reduced ΔB1 virus yield 12-fold compared to the ΔB1 virus yield in the HAP1 cells. Enzymatically active VRK2A rescued ΔB1 virus yield 3.1-fold but was still 3.9-fold short of the ΔB1 virus yield in the HAP1 cells. Enzymatically active VRK2B, catalytically inert VRK2A, and catalytically inert VRK2B failed to rescue the ΔB1 virus yield in the VRK2KO cells (9.6-, 10-, and 12-fold reductions, respectively, compared to the ΔB1 virus yield in the HAP1 cells). These results confirm and extend the evidence that VRK2 complements vaccinia virus replication in the absence of B1 by inhibiting B12. Specifically, these data designate VRK2A as a cellular kinase responsible for the phosphorylation of an unknown substrate that leads to the inhibition of B12's repressive activity and allows for vaccinia viral replication factory formation to proceed in the absence of B1. Lastly, the inability of VRK2B to perform the same kinase function as B1 and VRK2A highlights the importance of the VRK2 C terminus and, potentially, membrane localization during the phosphorylation event.

**B1 enzymatic activity is required to promote ΔB1 virus replication in VRK2KO cells.** To examine whether enzymatic activity is also required for B1 to inhibit B12, viral DNA accumulation and yield were determined in HAP1 and VRK2KO cells stably expressing either enzymatically active or catalytically inert B1. 3×FLAG-tagged enzymatically active and catalytically inert B1 constructs were generated as described above and stably expressed in VRK2KO cells (Fig. 11A and C). Enzymatically active and catalytically inert B1 constructs were expressed at comparable levels as determined by FLAG immunoblotting (Fig. 11C).

Next, viral DNA accumulation and yield were determined in parental HAP1 and VRK2KO cells stably expressing B1 that were infected with either WT or ΔB1 vaccinia virus (Fig. 11E). At 24 hpi, WT vaccinia virus DNA accumulation was unaffected by the deletion of VRK2 or the expression of either B1 construct (Fig. 11E, left). However, ΔB1 virus DNA accumulation in the VRK2KO cells was reduced 3.3-fold compared to its accumulation in ΔB1 virus-infected HAP1 cells. DNA accumulation in the VRK2KO cells expressing enzymatically active B1 was increased 7.3-fold compared to the accumulation in ΔB1 virus-infected VRK2KO cells and was 2.2-fold higher than that of ΔB1 virus-infected HAP1 cells. In contrast, the ΔB1 virus DNA accumulation in VRK2KO cells expressing catalytically inert B1 was not significantly different than the ΔB1 virus DNA accumulation in VRK2KO cells and was 2.5-fold reduced compared to the ΔB1 virus DNA accumulation in HAP1 cells. The viral yield of WT virus was unaffected by the deletion of VRK2 or the expression of either B1 construct (Fig. 11E, right). The viral yield of ΔB1 virus for each condition closely resembled the DNA accumulation results (Fig. 11E, right). The ΔB1 viral yield was reduced 4.9-fold by VRK2 deletion compared to the yield in HAP1 cells. Enzymatically active B1 rescued the ΔB1 virus yield in the VRK2KO cells 122-fold, surpassing the viral yield in the parental HAP1 cells, whereas catalytically inert B1 failed to increase the viral titer compared to that in VRK2KO cells. These results further highlight the requirement of a phosphorylation event that inhibits B12's repressive activity, directly or indirectly, in the absence of B1 and VRK2.

**FIG 11** Legend (Continued)
transduction followed by selection. FLAG and tubulin immunoblot analysis of transduced cell lysates for detection of exogenous FLAG-tagged B1 protein is shown. (D) DNA accumulation (left) and viral yield (right) measured for WT or ΔB1 virus at 24 hpi in HAP1 control or VRK2KO cell lines transduced with catalytically active and catalytically inert (kinase dead [KD]) variants of VRK2A or VRK2B at an MOI of 3. (E) DNA accumulation (left) and viral yield (right) measured for WT or ΔB1 virus at 24 hpi in HAP1 control or VRK2KO cell lines transduced with catalytically active and catalytically inert variants of B1 at an MOI of 3. ns, $P > 0.05$; *, $P < 0.05$; **, $P < 0.01$; ***, $P < 0.001$; ****, $P < 0.0001$.

## DISCUSSION

It is increasingly clear that mimicry of host cellular proteins is integral to the strategy poxviruses employ as these pathogens dysregulate host signaling pathways and promote viral replication. In one example, the high similarity of the vaccinia virus B1 kinase to the VRK family of host enzymes allows poxviruses to modulate multiple signal transduction pathways that are also governed by these host kinases. Recently, VRK2 has been shown to complement some of the modulatory functions of B1 during infections by vaccinia virus lacking B1 (15). Currently, much remains to be elucidated regarding the convergent roles of B1 and VRK2 functions in promoting vaccinia virus replication. Herein, we examined in detail the vaccinia virus replication block that results from the absence of B1 and VRK2, revealing novel insights into the importance of these factors for the early stages of DNA replication in a pathway antagonized by the vaccinia virus B12 pseudokinase.

As the vaccinia virus protein kinase B1 is highly conserved among many poxviruses but has no clear homologs within other virus families, we began our studies by positing that VRK2 may impact infection of other DNA viruses, as we had previously seen with the vaccinia virus B1 deletion mutant. We thus examined whether VRK2 deletion affected the viral replication of two other DNA viruses in addition to vaccinia virus. As we have previously reported, ΔB1 vaccinia virus replication was significantly decreased by VRK2 deletion in terms of DNA replication and viral yield. However, it is important to note that while the ΔB1 virus DNA replication at 24 hpi was near the WT virus levels in parental HAP1 cells, the viral yield from ΔB1-infected HAP1 cells was substantially decreased compared to the WT viral yield in the same cell type, demonstrating that VRK2 is unable to complement all the functions of B1 in promoting vaccinia virus replication. When we next examined the impact of VRK2 deletion on the replication of other DNA viruses, we found that viral sensitivity to VRK2 deletion was unique to vaccinia virus and occurred only in the context of B1 deletion, as VRK2 deletion did not affect the viral replication of either a representative herpesvirus or an adenovirus.

As vaccinia virus was the only DNA virus found to require B1 or VRK2, we posited that B1 and VRK2 may be acting via a pathway controlled by a vaccinia virus protein(s). The possibility that B1 and VRK2 were acting on vaccinia virus B12 was particularly intriguing, as B12 has been demonstrated recently to repress vaccinia virus DNA replication in a B1-dependent manner (6). In testing this theory, we found that ΔB1mutB12 vaccinia virus, which expresses a truncated form of vaccinia virus B12, replicated much more efficiently than ΔB1 virus in cells lacking VRK2 and equally well in parental HAP1 cells. These functional data indicate that, without B12, the ΔB1mutB12 lifecycle can proceed in a VRK2-independent manner and are consistent with a model in which B1 and VRK2 inhibit the repressive activity of B12 (Fig. 12).

We additionally confirmed that the sensitivity of vaccinia virus to B1- and VRK2-regulated B12 repression is not unique to HAP1 cells; viral replication in primary NHDF cells also displayed evidence of B12-mediated repression in the absence of B1 and VRK2. The recapitulation of the B1- and VRK2-dependent phenotype of vaccinia virus replication in NHDF cells is important and establishes a role for B1 and VRK2 in promoting vaccinia virus replication through inhibition of B12's repressive activity in nontransformed primary cells.

Next, to investigate the molecular mechanism underlying the functional link between vaccinia virus B1, cellular VRK2, and vaccinia virus B12, we assessed the interaction of B1 and VRK2 with B12. Immunofluorescence analysis of FLAG-tagged VRK2A and VRK2B with HA-tagged B12 revealed colocalization of VRK2A and VRK2B with B12 in infected and uninfected cells. Despite colocalization of both VRK2A and VRK2B with B12, protein immunoprecipitations identified VRK2A, but not VRK2B, as a robust interactor of B12. We found these results somewhat surprising, as they indicate that, despite complete identity to the N terminus of VRK2A and having localization more akin to that of B12, VRK2B does not interact with B12 to the extent that VRK2A does. Additionally, despite functional data demonstrating inhibition of B12's repressive ac-
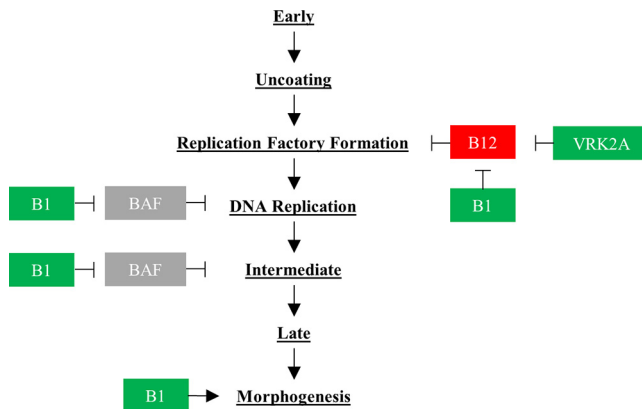
**FIG 12** Model for B12 inhibitory activity. The vaccinia virus B1 and cellular VRK2A kinases inhibit the repressive activity of the vaccinia virus B12 pseudokinase on viral replication factory formation. While VRK2A complements this function of B1, other functions of B1, such as B1's modulation of BAF, are not complemented by VRK2A. Direct interactions are indicated with black lines.

tivity by B1, we were unable to demonstrate reproducible coimmunoprecipitation of B1 and B12. Given the nature of kinase/substrate interactions, it is feasible that the interaction of B1 with B12 may be more transient than that of VRK2A, resulting in our inability to detect interaction of B1 and B12 using the methods applied. Further investigation will be needed to determine if interaction of B1 and B12 may be measurable with other assays.

Having established that B1 and VRK2 are able to inhibit B12's repressive activity but lacking any obvious functional roles for B12, we next utilized ΔB1 virus infection of VRK2KO cells to identify the execution point for B12's repressive activity. Although the presence of B12 correlates with impaired ΔB1 viral DNA replication in the absence of B1 and VRK2, poxviruses undergo numerous steps of their viral life cycle prior to undergoing viral DNA replication, any of which could be the execution point for B12. Therefore, we sought to determine the earliest stage of the vaccinia virus life cycle at which we could observe an effect on ΔB1 virus from VRK2 deletion.

The vaccinia virus protein kinase B1 and cellular protein kinase VRK2 have each been implicated in the regulation of several viral or cellular processes; thus, we sought to determine if any of the known roles of B1 or VRK2 coincided with the execution point of B12. Among the characterized B1 interactors, B1 has been shown to interact with and modulate several proteins involved in protein translation, including RACK1 (receptor for activated C kinase 1), ribosomal protein Sa, and ribosomal protein S2 (10, 37). Therefore, we sought to determine if B12 may be inhibiting early protein expression, perhaps by antagonizing B1-mediated ribosome customization, using both immunoblot analysis and mass spectrometry-assisted quantitation of early proteins. Aberrant gaps in early protein expression were not observed during ΔB1 virus infection of VRK2KO cells compared to the results for infections benefiting from either B1 or VRK2 activity, even with the identification of 79 of 117 early proteins. These data provided compelling evidence that the execution point for B12 during vaccinia virus infection occurs after early protein expression has occurred.

B1 has additionally been studied with reference to vaccinia virus uncoating. Specifically, an siRNA screen for the vaccinia virus genome-uncoating factor revealed B1 as a viral factor critical in vaccinia virus progression from early to intermediate gene expression (36). While D5 was revealed to be the vaccinia virus genome-uncoating factor in those studies, we posited that B1 may promote vaccinia virus uncoating in a B12-dependent manner in VRK2KO cells, as recent studies have identified that additional VACV uncoating proteins, including C5 and M2, exist as well (38). Interestingly, VRK2 has been demonstrated to modulate aspects of the unfolded protein response and proteasome (39–41), a cellular process required for vaccinia virus uncoating (33,

42). Therefore, we theorized that B1 and VRK2 may carry out complementary roles to regulate B12 during vaccinia virus uncoating. To determine if vaccinia virus uncoating was repressed by B12, we assessed vaccinia virus core activation and dissolution during ΔB1 virus infection of VRK2KO cells. However, our examination of STAT1 phosphorylation during ΔB1 virus infections of both HAP1 and VRK2KO cells did not support a model in which B1 and VRK2 function to assist vaccinia virus core activation. Additionally, using A4 core immunofluorescence analysis, VRK2 deletion was observed to have no effect on ΔB1 virus core dissolution. Together, these data are consistent with a model for the execution point of B12 occurring after vaccinia virus uncoating.

Lastly, as a sensitive measurement of vaccinia virus DNA replication initiation, we evaluated vaccinia virus replication factory formation in HAP1 or VRK2KO cells infected with WT and ΔB1 viruses. Replication factory formation in ΔB1 virus-infected VRK2KO cells revealed that this infection was impeded at the level of replication factory assembly, whereas replication factory assembly in a ΔB1 virus infection of HAP1 cells was indistinguishable from that of a WT infection. Cumulatively, these data indicate a role for B12 in repressing vaccinia virus replication factory assembly at the earliest stages of their formation.

Finally, we determined which properties of B1 or VRK2 were required for their inhibition of B12. For these studies, we employed exogenous complementation experiments with enzymatically active and catalytically inert VRK2A, VRK2B, and B1. Comparisons of viral DNA replication revealed that both enzymatically active B1 and VRK2A, but not enzymatically active VRK2B or any catalytically inert construct, were effective at inhibiting B12's repressive activity and promoting ΔB1 virus DNA replication. Together, these data support a model in which an unknown substrate, potentially B12 itself, is phosphorylated by B1 or VRK2A, resulting in inhibition of B12's repressive activity (Fig. 12).

It is intriguing that, despite near identity to VRK2A, enzymatically active VRK2B was unable to rescue ΔB1 virus from B12-mediated DNA replication repression. Previous studies comparing VRK2A and VRK2B have described differences in substrates and interacting proteins between VRK2 isoforms that were largely ascribed to result from their divergent localizations (30, 43–46). Therefore, as B12 is predominately nuclear in its expression, as is VRK2B, the inability of VRK2B to inhibit B12's repressive activity or interact with B12 was an unexpected observation and highlighted the importance of localization for B1 and VRK2A in the inhibition of B12's repressive activity. Expanded further, the inhibition of B12's repressive activity by B1 and VRK2A but not VRK2B may implicate the pool of cytoplasmic B12, as well as nuclear B12, as being important for repression of vaccinia virus DNA replication.

Though both enzymatically active B1 and VRK2A rescued ΔB1 virus from DNA replication-inhibitory B12 activity, it is noteworthy that enzymatically active B1 was significantly more effective at rescuing ΔB1 viral yields. In fact, enzymatically active B1 rescued the ΔB1 viral yield to the WT virus level, whereas enzymatically active VRK2A was only able to rescue the ΔB1 viral yield to near the yield observed from parental HAP1 cells. The inability of enzymatically active VRK2A to fully rescue the ΔB1 viral yield to the WT virus level is consistent with a model in which enzymatically active VRK2A can complement B1 in its inhibition of B12's repressive activity; however, VRK2A is unable to complement B1 in all its functions. This working model, in which VRK2A complements some but not all functions of B1 (Fig. 12), is also informed by previous evidence that BAF phosphorylation is unaffected by VRK2 deletion (15). However, while BAF phosphorylation was not altered by VRK2 deletion, VRK1 has been demonstrated to phosphorylate BAF, as is seen with B1 (23). Together, these data imply that when considered collectively, the cellular VRK family of proteins may perform all the functions of B1, but not when considered individually.

Returning to B12, we have further confirmed a functional link between B1 and B12 by demonstrating that a cellular homolog of B1, VRK2A, also inhibits B12-mediated repression of vaccinia virus DNA replication. The existence of a VRK2A-B12 signaling axis also contributes to our interpretation of previous studies of orf virus (ORFV).

Specifically, in those studies of ORFV, a *Poxviridae* family member lacking B1, ORFV replication was demonstrated to be independent of VRK2 (15). Those data revealed that a gap existed in our understanding of B1-mediated signaling that may now be resolved with the proposed model for VRK2 complementation of vaccinia virus via inhibition of B12's repressive activity. Specifically, ORFV lacks homologs of both B1 and B12, thereby offering a likely explanation as to why VRK2 is nonessential for ORFV replication.

Cumulatively, these data demonstrate that vaccinia virus B12 functions to repress vaccinia virus replication factory formation and that this function is masked not only by vaccinia virus B1 but also by the cellular kinase VRK2A in a phosphorylation-dependent manner. Together with previously published evidence, our studies demonstrate that B1 acts to promote vaccinia virus at multiple junctures of the vaccinia virus life cycle and that VRK2A complements some of these functions. Future evaluation of the B1/VRK2A/B12 signaling axis will be critical for dissecting the underlying mechanism of action for B12, as well as shedding light on how B1 and VRK2A mask the activity of B12. More broadly speaking, it is striking that VRK2 is the second VRK family member to have contributed to our understanding of B1-mediated signaling after studies of B1/VRK1 complementation revealed the antiviral function and phosphoregulation of BAF. Considering both the data herein and previous work on the B1/VRK1/BAF signaling axis, it is fascinating that, as first hypothesized by Nezu et al. over 20 years ago (21), B1 combines attributes of two of its cellular homologs in its regulation of the poxvirus life cycle.

## MATERIALS AND METHODS

**Cell culture.** Human near-haploid fibroblast HAP1 parental and vaccinia virus-related kinase 2 knockout (VRK2KO) cells were obtained from Horizon Genomics, maintained in Iscove's modified Dulbecco's medium (IMDM) supplemented with 10% fetal bovine serum (FBS; Atlanta Biologicals) and penicillin-streptomycin, and incubated at 37°C in a 5% $CO_2$ atmosphere. VRK2KO cells contain a 7-bp deletion in VRK2 exon 2. Human neonatal dermal fibroblast NHDF cells were obtained from Lonza, maintained in Dulbecco's modified Eagle's medium (DMEM) supplemented with 2% FBS and penicillin-streptomycin, and incubated at 37°C in a 5% $CO_2$ atmosphere. African green monkey kidney CV-1 cells purchased from Invitrogen Life Technologies, African green monkey kidney Vero cells purchased from ATCC, human kidney 293T cells purchased from ATCC, African green monkey kidney BSC40 cells purchased from ATCC, and human kidney 293 cells courtesy of Frank Graham (AdVec, Inc.) were all maintained in DMEM supplemented with 10% FBS and penicillin-streptomycin and incubated at 37°C in a 5% $CO_2$ atmosphere.

**Viruses and viral infections.** Wild-type vaccinia virus (WR strain), B1 deletion mutant virus (ΔB1) (15), adapted B1 deletion mutant virus (ΔB1mutB12) (6), WRHAB12 virus (6), D5-deficient Cts24 virus, and E9-deficient Cts42 virus were used for vaccinia virus infections. These viruses were expanded on BSC40, CV-1, or CV-1B1MYC cells, purified using a sucrose cushion, and stored at −80°C in 1 mM Tris, pH 9. HSV-1, strain KOS, and Ad5 (ATCC), strain Adenoid 75, were additionally used for these studies. HSV-1, strain KOS, was expanded on Vero cells, purified using a sucrose cushion, and stored at −80°C in cell culture medium. Ad5 was expanded on 293 cells, purified by two sequential CsCl gradients, desalted, and stored at −80°C in 20 mM Tris, 100 mM NaCl, 1mM $MgCl_2$, 10% glycerol. Ad5 virus particle quantity was determined on a NanoDrop Lite spectrophotometer (Thermo Scientific) with optical density at 260 nm ($OD_{260}$).

For vaccinia viral DNA accumulation and viral titer determination, cells (NHDF [$2.3 \times 10^5$] or HAP1 and VRK2KO [$6.9 \times 10^6$] cells) were infected with WT, ΔB1, or ΔB1mutB12 virus at a multiplicity of infection (MOI) of 3 PFU per cell at 37°C for 24 h. Cells were harvested into 400 $\mu$l phosphate-buffered saline (PBS). Cells were aliquoted (200 $\mu$l for viral DNA accumulation and 200 $\mu$l for viral titer determination) prior to downstream assays. For viral yield assays, following cell harvest, cells were pelleted and resuspended in 200 $\mu$l 10 mM Tris (pH 9). Virus samples were freeze-thaw lysed three times and titrated on CV-1 cells or CV-1B1MYC cells.

For HSV-1 viral titer determination, cells (HAP1 and VRK2KO cells [$6.9 \times 10^6$]) were infected with KOS virus at an MOI of 0.1 PFU/cell at 37°C for 72 h. Viral supernatant was collected and freeze-thaw lysed three times before titration on Vero cells.

For adenovirus DNA accumulation determination, cells (HAP1 and VRK2KO cells [$2.6 \times 10^6$]) were infected with Ad5 at an MOI of 500 virus particles per cell at 37°C for 48 h. Cells were harvested into 100 $\mu$l PBS. Amounts of 50 $\mu$l were used for DNA extraction.

For immunofluorescence of infected cells, cells were infected with WT, ΔB1, WRHAB12, Cts24, or Cts42 vaccinia virus at an MOI of 5 PFU/cell at 39.7°C or 37°C for the indicated times prior to fixation with 4% paraformaldehyde.

For protein immunoprecipitations, immunoblotting, and proteomic analysis of vaccinia virus-infected cells, cells were infected with vaccinia virus at the indicated MOIs and times prior to lysate collection.

For STAT-1 dephosphorylation assays, cells were infected with vaccinia virus at an MOI of 2.5 or 5 for 1 h prior to IFN-$\gamma$ treatment (50 U/ml) for 0.5 h, followed by lysate collection.

**Mutagenesis and cloning of VRK2, B1, and B12 expression vectors.** pHAGE-HYG-1XFLAGVRK2A and pHAGE-HYG-1XFLAGVRK2B constructs were produced by amplifying the VRK2 open reading frame (ORF) using the primers FBamHI-Kozak-FLAG-VRK2 (5′-TTCTGGATCCGCTAGCGCCACCATGGATTACAAGG ATGACGATGACATGCCACCAAAAAGAAATG-3′) and RVRK2A-BamHI (5′-GCGCGGATCCTCAGAGAAAAAATA AAGCAAGAAATACTAACATCAAAAGGACAGG-3′) or RVRK2B-BamHI (5′-TCTCGGATCCTCAATAGCCTAAGCT TCTACCCTGAGCTGCTTCATTGTTC-3′) and cloning the products into the BamHI site of the multiple cloning site of the pHAGE-HYG-MCS vector (47). pHAGE-HYG-1XFLAGKDVRK2A and pHAGE-HYG-1XFLAGKDVRK2B constructs were produced using overlap PCR mutagenesis of both the ATP binding site (mutating K at position 61 to A [K61A]) and catalytic site (D186G) of VRK2 using outside primers and one set of the internal mutagenesis primers FK61AVRK2 (5′-GCAAGACATGTAGTAGCCGTGGAATATCAAG-3′), RK61AVRK2 (5′-CTTGATATTCCACGGCTACTACATGTCTTGC-3′), FD186GVRK2 (5′-CCAGGTTTATCTTGCAGG GTATGGACTTTCC-3′), and RD186GVRK2 (5′-GGAAAGTCCATACCCTGCAAGATAAACCTGG-3′) and cloning the products into the BamHI site of the multiple cloning site of the pHAGE-HYG-MCS vector. pHAGE-HYG-3XFLAGVRK2A and pHAGE-HYG-3XFLAGVRK2B were produced using overlap PCR by amplifying the VRK2 ORF and the 3×FLAG sequence separately using the primers FFLAG (5′-GAGAGGATCCGCCACCA TGGACTACAAAGACCATGACGG-3′), FFLAG+VRK2 (5′-TGACATCGATTACAAGGATGACGATGACATGCCACC AAAAAGAAATG-3′), RFLAG+VRK2 (5′-CATTTCTTTTTGGTGGCATGTCATCGTCATCCTTGTAATCGATGTCA-3′), and RVRK2A-BamHI (above) or RVRK2B-BamHI (above) and cloning the products into the BamHI site of the multiple cloning site of pHAGE-HYG-MCS vector. pHAGE-HYG-3XFLAGB1 was produced using overlap PCR by amplifying a codon-optimized B1 ORF (15) and the 3×FLAG sequence separately using the primers FFLAG (above), FFLAG+B1 (5′-TGACATCGATTACAAGGATGACGATGACATGAACTTCCAAGGC TTGG-3′), RFLAG+B1 (5′-CCAAGCCTTGGAAGTTCATGTCATCGTCATCCTTGTAATCGATGTCA-3′), and RB1-BamHI (5′-GCGCGGATCCTCAATAGTAAACTCCTTGCATGAGAATGTGGCGAAACTCGTCATAATT-3′) and cloning the product into the BamHI site of the multiple cloning site of the pHAGE-HYG-MCS vector. pHAGE-HYG-3XFLAGKDB1 was produced using overlap PCR mutagenesis of both the ATP binding site (K41A) and catalytic site (D167G) of B1 using outside primers and one set of the internal mutagenesis primers FK41AB1 (5′-CAATTACGTCGTCGCCATTGAGCCTAAGGC-3′), RK41AB1 (5′-GCCTTAGGCTCAATGGC GACGACGTAATTG-3′), FD167GB1 (5′-GCTGTATCTCGTGGGGTATGGGTTGGTGTCC-3′), and RD167GB1 (5′-GGACACCAACCCATACCCCACGAGATACAGC-3′) and cloning the products into the BamHI site of the multiple cloning site of the pHAGE-HYG-MCS vector. pHAGE-PURO-HAB12 was produced by amplifying a codon-optimized, HA-tagged B12 ORF (6) using the primers FBamHI-Kozak-HAB12 (5′-GAGAGAGGAT CCGCCACCATGTATCCCTACGACG-3′) and RB12-BamHI (5′-GAGAGAGGATCCTTAGTCCTGGATGAACAGCTT CCGC-3′) and cloning the product into the BamHI site of the multiple cloning site of the pHAGE-PURO-MCS vector. A pHAGE-HYG-GFPHA control construct was additionally produced by amplifying a green fluorescent protein (GFP) ORF using the primers FBamHI-KOZAK-GFP (5′-TATATAGGATCCGCCACCATGG TGAGCAAGGGCGAGGAGCTGTTCACC-3′) and RGFPHA-BamHI (5′-GAGAGAGGATCCGGCGTAGTCGGGCAC GTCGTAGGGATACTTGTACAGCTC-3′) and cloning the product into the BamHI site of the multiple cloning site of the pHAGE-HYG-MCS vector. All constructs were verified by DNA sequencing.

**Generation of stable cells expressing VRK2, B1, and B12.** Lentiviral expression vectors for the respective proteins were used to generate lentiviruses as described previously (15). For transduction, HAP1 or VRK2KO cells were seeded in 35-mm dishes at $2.3 \times 10^5$. The next day, cell growth medium was replaced with 1 ml of lentivirus supernatant and incubated for 16 h. The medium was then replaced with fresh medium and incubated for an additional 24 h. Cells were then passaged in medium containing 500 $\mu$g/ml (HAP1 and VRK2KO cells) of hygromycin and/or 0.5 $\mu$g/ml of puromycin (HAP1 and VRK2KO cells) to select for stable lentiviral integration. Protein expression was confirmed by immunoblotting using mouse anti-FLAG, mouse anti-VRK2, or mouse anti-HA antibody.

**DNA purification and qPCR.** Vaccinia viral DNA was extracted using the GeneJET whole-blood genomic DNA purification minikit (Thermo Scientific) following the manufacturer's protocol. Vaccinia viral DNA qPCR was performed using iTaq universal SYBR green supermix (Bio-Rad) by following a protocol described previously (17). Serial dilutions were included in each qPCR run to develop a standard curve and determine the PCR efficiency of the primer sets in each experiment. qPCR analysis was performed using approximately 10 ng DNA and 1 $\mu$M each primer. DNA quantification used primers FHA (5′-CATCATCTGGAATTGTCACTACTAAA-3′) and RHA (5′-ACGGCCGACAATTATAATTAATGC-3′).

Ad5 viral DNA was extracted using the PureLink viral RNA/DNA minikit (Invitrogen) following the manufacturer's protocol. Ad5 viral DNA qPCR was performed using SYBR green PCR master mix (Applied Biosystems). qPCR analysis was performed using approximately 1.5 $\mu$g DNA and 0.2 $\mu$M each primer. DNA quantification used primers FHexon (5′-TTCGATGATGCCGCAGTGGTCTTACATGCAC-3′) and RHexon (5′-TTTCTAAACTTGTTATTCAGGCTGAAGTACG-3′). The results were compared to a standard curve created by dilution of pCR2.1-TOPO vector (Invitrogen) containing the Ad5 hexon fragment. The results were then converted to number of copies per cell.

**siRNA depletion.** Small interfering RNAs (siRNAs) against VRK2 (both isoforms) and nontargeting siRNAs were designed and ordered from Dharmacon. The siRNA sequences were as follows: siVRK2, 5′-CACAAUAGGUUAAUCGAAAUU-3′, and nontargeting siRNA, 5′-CAGUCGCGUUUGCGACUGGUU-3′. NHDF cells were transfected with 100 nM siRNA using Lipofectamine RNAiMax (Life Technologies) following the manufacturer's protocol. Protein depletion was measured by immunoblot analysis at 3 days posttransfection. For viral infections in siRNA-treated cells, cells were split into 6-well plates 3 days posttransfection and infected 4 days posttransfection, prior to DNA accumulation and viral yield assays.

**Immunoblotting.** To evaluate protein expression, cells were harvested, pelleted, and suspended in SDS sample buffer supplemented with protease and phosphatase inhibitors and nuclease. Lysates were resolved on 10% (STAT-1 and pSTAT-1) or 12% (VRK2, B1, I3, H5, D5, F17, and tubulin) SDS-PAGE gels and

transferred to polyvinylidene difluoride (PVDF) membranes. The primary antibodies used were antibodies to the following proteins and used at the indicated dilutions: $\beta$-tubulin, 1:10,000 (T7816; Sigma); pSTAT-1, 1:1,000 (D4A7; Cell Signaling); STAT-1, 1:500 (HPA000982; Sigma); FLAG, 1:5,000 (F1804; Sigma); VRK2, 1:1250 (ab58052; Abcam); VRK2, 1:5,000 (sc365199; Santa Cruz); I3, 1:10,000 (custom) (48); D5, 1:500 (custom) (49); H5, 1:10,000 (custom) (50); HA, 1:1,000 (901514; BioLegend); HA, 1:1,000 (C29F4; Cell Signaling); and F17, 1:6,000 (custom) (51).

**Immunofluorescence assays.** For I3 immunofluorescence analysis, HAP1 or VRK2KO cells were fixed in 4% paraformaldehyde in PBS and permeabilized with 0.2% Triton X-100 in PBS for 10 m. Cells were then incubated with anti-I3 antibody, 1:300 (custom), for 1 h. Cells were washed with PBS followed by incubation with Alexa Fluor 594-conjugated secondary antibody for 1 h. As described previously for core integrity assays, cells were fixed in 4% paraformaldehyde and permeabilized with 0.1% saponin for 30 m. Cells were blocked with 10% goat serum for 1 h. Anti-A4 antibody, 1:500 (custom) (34), in 10% goat serum, 0.1% saponin was used for primary staining. Cells were washed with PBS, followed by incubation with Alexa Fluor 488-conjugated secondary antibody in 10% goat serum, 0.1% saponin. FLAG and HA immunofluorescence analysis was performed on VRK2KO cells expressing 3XFLAGVRK2A or 3XFLAGVRK2B with and without HAB12. Cells were fixed in 4% paraformaldehyde and permeabilized with 0.2% Triton X-100 for 10 min. Cells were then incubated with anti-HA antibody, 1:400 (901514; BioLegend), and anti-FLAG antibody, 1:400 (740001; Thermo Fisher), for 2 h. Cells were washed with PBS followed by incubation with Alexa Fluor-conjugated secondary antibodies for 2 h. Fluorescence images were acquired on an inverted confocal microscope (Nikon A1R) and quantified and/or equivalently edited with Image J software.

**Protein immunoprecipitations.** To study VRK2, B1, and B12 interactions, cells (uninfected or 7 hpi) were harvested in cold PBS and pelleted. Cells were lysed with a lysis buffer containing 50 mM Tris-HCl, pH 7.4, 150 mM NaCl, 1% Triton X-100 and supplemented with protease and phosphatase inhibitors and nuclease. B1/VRK2 or B12 and their interacting proteins were pulled down with anti-FLAG M2 antibody magnetic beads (Sigma) or anti-HA antibody magnetic beads (Cell Signaling), eluted in SDS sample buffer supplemented with protease and phosphatase inhibitors by heating at 95°C for 5 m, and then subjected to protein immunoblotting.

**Proteomic analysis of infected cells.** To determine early protein expression levels, infected cells (HAP1 and VRK2KO, [$6.9 \times 10^6$]) were harvested in PBS. One half of the cell pellet was lysed with radioimmunoprecipitation assay (RIPA) buffer (Thermo Scientific). Proteins from infected cell lysates were precipitated using ProteoExtract (Calbiochem) following the manufacturer's protocol, dissolved, and assayed for total protein concentration using the CB-X kit (GBiosciences). Proteins (25 $\mu$g) were then reduced, alkylated, and digested with trypsin. An amount of 0.5 $\mu$g of each was then analyzed by nanoscale LC-MS/MS using a 2-h gradient on a 0.075-mm by 250-mm $C_{18}$ column feeding into a Q-Exactive HF mass spectrometer. All MS/MS samples were analyzed using Mascot (Matrix Science). Mascot was set up to search the Swiss-Prot database (*Homo sapiens* reference proteome, release 2018_07, 20,387 entries) and the UniProt database (vaccinia virus strain WR reference proteome, release 2017_11, 217 entries) with added contaminants assuming the digestion enzyme trypsin. Mascot was searched with a fragment ion mass tolerance of 0.060 Da and a parent ion tolerance of 10.0 ppm. Deamination of asparagine and glutamine, oxidation of methionine, and phosphorylation of serine, threonine, and tyrosine were specified in Mascot as variable modifications. Scaffold software was used to validate MS/MS-based peptide and protein identifications. Peptide identifications were accepted if they could be established at greater than 80% probability by the Peptide Prophet algorithm with Scaffold delta-mass correction. Protein identifications were accepted if they could be established at greater than 99% probability and contained at least two identified peptides. Protein probabilities were assigned by the Protein Prophet algorithm. Proteins that contained similar peptides and could not be differentiated based on MS/MS analysis alone were grouped to satisfy the principles of parsimony. Proteins sharing significant peptide evidence were grouped into clusters. Protein identifications were compared to the vaccinia virus WR reference proteome (UniProt) and assessed for the presence or absence of each respective protein. The vaccinia virus WR reference proteome was categorized into early, intermediate, or late gene expression classes using transcriptome profiling from Yang et al. (31). The experiment was performed in duplicate.

**Statistics.** Experiments were repeated at least in triplicate unless otherwise noted, and graphed data represent the means of data from all experimental replicates. Error bars shown in the figures represent one standard deviation from the mean. The $P$ values indicated in the figures were calculated by one-way analysis of variance (ANOVA) or two-tailed Student's $t$ test using Prism version 8.00 for Windows (GraphPad).

## SUPPLEMENTAL MATERIAL

Supplemental material for this article may be found at https://doi.org/10.1128/JVI .00855-19.

**SUPPLEMENTAL FILE 1**, XLSX file, 0.04 MB.

## ACKNOWLEDGMENTS

We thank the University of Nebraska-Lincoln Center for Biotechnology for help with microscopy and proteomic methodologies.

## REFERENCES

1. Moss B. 2013. Poxviridae, p 2129–2159. In Knipe DM, Howley PM (ed), Fields virology, 6th ed, vol 2. Lippincott Williams and Wilkins, Philadelphia, PA.
2. Traktman P, Anderson MK, Rempel RE. 1989. Vaccinia virus encodes an essential gene with strong homology to protein kinases. J Biol Chem 264:21458–21461.
3. Graham SC, Bahar MW, Cooray S, Chen RA, Whalen DM, Abrescia NG, Alderton D, Owens RJ, Stuart DI, Smith GL, Grimes JM. 2008. Vaccinia virus proteins A52 and B14 share a Bcl-2-like fold but have evolved to inhibit NF-kappaB rather than apoptosis. PLoS Pathog 4:e1000128. https://doi.org/10.1371/journal.ppat.1000128.
4. Banadyga L, Gerig J, Stewart T, Barry M. 2007. Fowlpox virus encodes a Bcl-2 homologue that protects cells from apoptotic death through interaction with the proapoptotic protein Bak. J Virol 81:11032–11045. https://doi.org/10.1128/JVI.00734-07.
5. Beattie E, Tartaglia J, Paoletti E. 1991. Vaccinia virus-encoded eIF-2 alpha homolog abrogates the antiviral effect of interferon. Virology 183:419–422. https://doi.org/10.1016/0042-6822(91)90158-8.
6. Olson AT, Wang Z, Rico AB, Wiebe MS. 2019. A poxvirus pseudokinase represses viral DNA replication via a pathway antagonized by its paralog kinase. PLoS Pathog 15:e1007608. https://doi.org/10.1371/journal.ppat.1007608.
7. Ibrahim N, Wicklund A, Jamin A, Wiebe MS. 2013. Barrier to autointegration factor (BAF) inhibits vaccinia virus intermediate transcription in the absence of the viral B1 kinase. Virology 444:363–373. https://doi.org/10.1016/j.virol.2013.07.002.
8. Wiebe MS, Traktman P. 2007. Poxviral B1 kinase overcomes barrier to autointegration factor, a host defense against virus replication. Cell Host Microbe 1:187–197. https://doi.org/10.1016/j.chom.2007.03.007.
9. Jamin A, Ibrahim N, Wicklund A, Weskamp K, Wiebe MS. 2015. Vaccinia B1 kinase is required for post-replicative stages of the viral lifecycle in a BAF-independent manner in U2OS cells. J Virol 89:10247–10259. https://doi.org/10.1128/JVI.01252-15.
10. Jha S, Rollins MG, Fuchs G, Procter DJ, Hall EA, Cozzolino K, Sarnow P, Savas JN, Walsh D. 2017. Trans-kingdom mimicry underlies ribosome customization by a poxvirus kinase. Nature 546:651–655. https://doi.org/10.1038/nature22814.
11. Kovacs GR, Vasilakis N, Moss B. 2001. Regulation of viral intermediate gene expression by the vaccinia virus B1 protein kinase. J Virol 75:4048–4055. https://doi.org/10.1128/JVI.75.9.4048-4055.2001.
12. Condit RC, Motyczka A, Spizz G. 1983. Isolation, characterization, and physical mapping of temperature-sensitive mutants of vaccinia virus. Virology 128:429–443. https://doi.org/10.1016/0042-6822(83)90268-4.
13. Rempel RE, Anderson MK, Evans E, Traktman P. 1990. Temperature-sensitive vaccinia virus mutants identify a gene with an essential role in viral replication. J Virol 64:574–583.
14. Rempel RE, Traktman P. 1992. Vaccinia virus B1 kinase: phenotypic analysis of temperature-sensitive mutants and enzymatic characterization of recombinant proteins. J Virol 66:4413–4426.
15. Olson AT, Rico AB, Wang Z, Delhon G, Wiebe MS. 2017. Deletion of the vaccinia virus B1 kinase reveals essential functions of this enzyme complemented partly by the homologous cellular kinase VRK2. J Virol 91:e00635-17. https://doi.org/10.1128/JVI.00635-17.
16. Ibrahim N, Wicklund A, Wiebe MS. 2011. Molecular characterization of the host defense activity of the barrier to autointegration factor against vaccinia virus. J Virol 85:11588–11600. https://doi.org/10.1128/JVI.00641-11.
17. Jamin A, Wicklund A, Wiebe MS. 2014. Cell and virus mediated regulation of the barrier-to-autointegration factor's phosphorylation state controls its DNA binding, dimerization, subcellular localization, and antipoxviral activity. J Virol 88:5342–5355. https://doi.org/10.1128/JVI.00427-14.
18. Segura-Totten M, Wilson KL. 2004. BAF: roles in chromatin, nuclear structure and retrovirus integration. Trends Cell Biol 14:261–266. https://doi.org/10.1016/j.tcb.2004.03.004.
19. Jamin A, Wiebe MS. 2015. Barrier to autointegration factor (BANF1): interwoven roles in nuclear structure, genome integrity, innate immunity, stress responses and progeria. Curr Opin Cell Biol 34:61–68. https://doi.org/10.1016/j.ceb.2015.05.006.
20. Wiebe MS, Jamin A. 2016. The barrier to autointegration factor: interlocking antiviral defense with genome maintenance. J Virol 90:3806–3809. https://doi.org/10.1128/JVI.00178-16.
21. Nezu J, Oku A, Jones MH, Shimane M. 1997. Identification of two novel human putative serine/threonine kinases, VRK1 and VRK2, with structural similarity to vaccinia virus B1R kinase. Genomics 45:327–331. https://doi.org/10.1006/geno.1997.4938.
22. Nichols RJ, Traktman P. 2004. Characterization of three paralogous members of the mammalian vaccinia related kinase family. J Biol Chem 279:7934–7946. https://doi.org/10.1074/jbc.M310813200.
23. Boyle KA, Traktman P. 2004. Members of a novel family of mammalian protein kinases complement the DNA-negative phenotype of a vaccinia virus ts mutant defective in the B1 kinase. J Virol 78:1992–2005. https://doi.org/10.1128/JVI.78.4.1992-2005.2004.
24. Nichols RJ, Wiebe MS, Traktman P. 2006. The vaccinia-related kinases phosphorylate the N′ terminus of BAF, regulating its interaction with DNA and its retention in the nucleus. Mol Biol Cell 17:2451–2464. https://doi.org/10.1091/mbc.e05-12-1179.
25. Howard ST, Smith GL. 1989. Two early vaccinia virus genes encode polypeptides related to protein kinases. J Gen Virol 70:3187–3201. https://doi.org/10.1099/0022-1317-70-12-3187.
26. Banham AH, Smith GL. 1993. Characterization of vaccinia virus gene B12R. J Gen Virol 74:2807–2812. https://doi.org/10.1099/0022-1317-74-12-2807.
27. Manning G, Whyte DB, Martinez R, Hunter T, Sudarsanam S. 2002. The protein kinase complement of the human genome. Science 298:1912–1934. https://doi.org/10.1126/science.1075762.
28. Boudeau J, Miranda-Saavedra D, Barton GJ, Alessi DR. 2006. Emerging roles of pseudokinases. Trends Cell Biol 16:443–452. https://doi.org/10.1016/j.tcb.2006.07.003.
29. Eyers PA, Murphy JM. 2013. Dawn of the dead: protein pseudokinases signal new adventures in cell biology. Biochm Soc Trans 41:969–974. https://doi.org/10.1042/BST20130115.
30. Blanco S, Klimcakova L, Vega FM, Lazo PA. 2006. The subcellular localization of vaccinia-related kinase-2 (VRK2) isoforms determines their different effect on p53 stability in tumour cell lines. FEBS J 273:2487–2504. https://doi.org/10.1111/j.1742-4658.2006.05256.x.
31. Yang Z, Reynolds SE, Martens CA, Bruno DP, Porcella SF, Moss B. 2011. Expression profiling of the intermediate and late stages of poxvirus replication. J Virol 85:9899–9908. https://doi.org/10.1128/JVI.05446-11.
32. Dower K, Rubins KH, Hensley LE, Connor JH. 2011. Development of vaccinia reporter viruses for rapid, high content analysis of viral function at all stages of gene expression. Antiviral Res 91:72–80. https://doi.org/10.1016/j.antiviral.2011.04.014.
33. Schmidt F, Bleck C, Reh L, Novy K, Wollscheid B, Helenius A, Stahlberg H, Mercer J. 2013. Vaccinia virus entry is followed by core activation and proteasome-mediated release of the immunomodulatory effector VH1 from lateral bodies. Cell Rep 4:464–476. https://doi.org/10.1016/j.celrep.2013.06.028.
34. Whitbeck JC, Foo CH, Ponce de Leon M, Eisenberg RJ, Cohen GH. 2009. Vaccinia virus exhibits cell-type-dependent entry characteristics. Virology 385:383–391. https://doi.org/10.1016/j.virol.2008.12.029.
35. Bengali Z, Townsley AC, Moss B. 2009. Vaccinia virus strain differences in cell attachment and entry. Virology 389:132–140. https://doi.org/10.1016/j.virol.2009.04.012.
36. Kilcher S, Schmidt FI, Schneider C, Kopf M, Helenius A, Mercer J. 2014. siRNA screen of early poxvirus genes identifies the AAA+ ATPase D5 as the virus genome-uncoating factor. Cell Host Microbe 15:103–112. https://doi.org/10.1016/j.chom.2013.12.008.
37. Banham AH, Leader DP, Smith GL. 1993. Phosphorylation of ribosomal proteins by the vaccinia virus B1R protein kinase. FEBS Lett 321:27–31. https://doi.org/10.1016/0014-5793(93)80614-Z.
38. Liu B, Panda D, Mendez-Rios JD, Ganesan S, Wyatt LS, Moss B. 2018. Identification of poxvirus genome uncoating and DNA replication factors with mutually redundant roles. J Virol 92:e02152-17.
39. Kim S, Lee D, Lee J, Song H, Kim HJ, Kim KT. 2015. Vaccinia-related kinase 2 controls the stability of the eukaryotic chaperonin TRiC/CCT by inhib-

iting the deubiquitinating enzyme USP25. Mol Cell Biol 35:1754–1762. https://doi.org/10.1128/MCB.01325-14.

40. Lee E, Ryu HG, Kim S, Lee D, Jeong YH, Kim KT. 2016. Glycogen synthase kinase 3beta suppresses polyglutamine aggregation by inhibiting vaccinia-related kinase 2 activity. Sci Rep 6:29097. https://doi.org/10.1038/srep29097.

41. Kim S, Park DY, Lee D, Kim W, Jeong YH, Lee J, Chung SK, Ha H, Choi BH, Kim KT. 2014. Vaccinia-related kinase 2 mediates accumulation of polyglutamine aggregates via negative regulation of the chaperonin TRiC. Mol Cell Biol 34:643–652. https://doi.org/10.1128/MCB.00756-13.

42. Mercer J, Snijder B, Sacher R, Burkard C, Bleck CK, Stahlberg H, Pelkmans L, Helenius A. 2012. RNAi screening reveals proteasome- and Cullin3-dependent stages in vaccinia virus infection. Cell Rep 2:1036–1047. https://doi.org/10.1016/j.celrep.2012.09.003.

43. Birendra K, May DG, Benson BV, Kim DI, Shivega WG, Ali MH, Faustino RS, Campos AR, Roux KJ. 2017. VRK2A is an A-type lamin-dependent nuclear envelope kinase that phosphorylates BAF. Mol Biol Cell 28:2241–2250. https://doi.org/10.1091/mbc.E17-03-0138.

44. Hirata N, Suizu F, Matsuda-Lennikov M, Tanaka T, Edamura T, Ishigaki S, Donia T, Lithanatudom P, Obuse C, Iwanaga T, Noguchi M. 2018. Functional characterization of lysosomal interaction of Akt with VRK2. Oncogene 37:5367–5386. https://doi.org/10.1038/s41388-018-0330-0.

45. Fernandez IF, Perez-Rivas LG, Blanco S, Castillo-Dominguez AA, Lozano J, Lazo PA. 2012. VRK2 anchors KSR1-MEK1 to endoplasmic reticulum forming a macromolecular complex that compartmentalizes MAPK signaling. Cell Mol Life Sci 69:3881–3893. https://doi.org/10.1007/s00018-012-1056-8.

46. Sanz-Garcia M, Vazquez-Cedeira M, Kellerman E, Renbaum P, Levy-Lahad E, Lazo PA. 2011. Substrate profiling of human vaccinia-related kinases identifies coilin, a Cajal body nuclear protein, as a phosphorylation target with neurological implications. J Proteomics 75:548–560. https://doi.org/10.1016/j.jprot.2011.08.019.

47. Mostoslavsky G, Fabian AJ, Rooney S, Alt FW, Mulligan RC. 2006. Complete correction of murine Artemis immunodeficiency by lentiviral vector-mediated gene transfer. Proc Natl Acad Sci U S A 103:16406–16411. https://doi.org/10.1073/pnas.0608130103.

48. Rochester SC, Traktman P. 1998. Characterization of the single-stranded DNA binding protein encoded by the vaccinia virus I3 gene. J Virol 72:2917–2926.

49. Evans E, Traktman P. 1987. Molecular genetic analysis of a vaccinia virus gene with an essential role in DNA replication. J Virol 61:3152–3162.

50. DeMasi J, Traktman P. 2000. Clustered charge-to-alanine mutagenesis of the vaccinia virus H5 gene: isolation of a dominant, temperature-sensitive mutant with a profound defect in morphogenesis. J Virol 74:2393–2405. https://doi.org/10.1128/jvi.74.5.2393-2405.2000.

51. Liu K, Lemon B, Traktman P. 1995. The dual-specificity phosphatase encoded by vaccinia virus, VH1, is essential for viral transcription in vivo and in vitro. J Virol 69:7823–7834.